Toxicology and Applied Pharmacology **176,** 34–53 (2001)
doi:10.1006/taap.2001.9274, available online at http://www.idealibrary.com on IDEAL®

Microarray Analysis of Differential Gene Expression in Lead-Exposed Astrocytes

Christopher M. L. S. Bouton,* Mir Ahamed Hossain,†,§ Laurence P. Frelin,§ John Laterra,*,†,‡,§ and Jonathan Pevsner*,§,[1]

**Department of Neuroscience, †Department of Neurology, and ‡Department of Oncology, Johns Hopkins University, Baltimore, Maryland 21205; and §Department of Neurology, Kennedy Krieger Institute, Baltimore, Maryland 21205*

Received May 14, 2001; accepted July 19, 2001

Microarray Analysis of Differential Gene Expression in Lead-Exposed Astrocytes. Bouton, C. M. L. S., Hossain, M. A., Frelin, L. P., Laterra, J., and Pevsner, J. (2001). *Toxicol. Appl. Pharmacol.* **176, 34–53.**

The toxic metal lead is a widespread environmental health hazard that can adversely affect human health. In an effort to better understand the cellular and molecular consequences of lead exposure, we have employed cDNA microarrays to analyze the effects of acute lead exposure on large-scale gene expression patterns in immortalized rat astrocytes. Our studies identified many genes previously reported to be differentially regulated by lead exposure. Additionally, we have identified novel putative targets of lead-mediated toxicity, including members of the family of calcium/phospholipid binding annexins, the angiogenesis-inducing thrombospondins, collagens, and tRNA synthetases. We demonstrate the ability to distinguish lead-exposed samples from control or sodium samples solely on the basis of large-scale gene expression patterns using two complementary clustering methods. We have confirmed the altered expression of candidate genes and their encoded proteins by RT–PCR and Western blotting, respectively. Finally, we show that the calcium-dependent phospholipid binding protein annexin A5, initially identified as a differentially regulated gene by our microarray analysis, is directly bound and activated by nanomolar concentrations of lead. We conclude that microarray technology is an effective tool for the identification of lead-induced patterns of gene expression and molecular targets of lead.

Key Words: **metal; toxicity; microarray; toxicogenomics.**

The natural properties of the heavy metal lead have made it an indispensable part of numerous industrial procedures. For decades, lead was used in automotive gasoline and household paints (Haar, 1975; Mushak and Crocetti, 1989; Goyer, 1996; Romieu *et al.*, 1997; Mielke and Reagan, 1998). Although use of lead in these products was made illegal in the United States decades ago, lead is still used in numerous industrial procedures (Johnson, 1998). Lead is used despite the fact that it is widely known to cause learning disabilities, behavioral abnormalities, and death in humans. As a result, lead is one of the most widely prevalent environmental causes of preventable neurological disorders (Landrigan and Todd, 1994).

Approximately 8.9% of children in the United States alone have blood-lead levels in excess of the 10 μg/dL ($\sim$0.5 μM) threshold determined to be "concerning" by the Centers for Disease Control (Centers for Disease Control, 1991; Goldstein, 1992; Needleman, 1994, 1998; Bressler *et al.*, 1999). Numerous bodily systems including the reproductive, nervous, gastrointestinal, immune, renal, cardiovascular, skeletal, muscular, and hematopoetic systems are affected by lead poisoning (Landrigan and Todd, 1994). Symptoms of chronic low-level lead exposure include learning disorders, IQ reduction, hyperactive behavior, ataxia, and convulsions (Needleman *et al.*, 1990; Bressler and Goldstein, 1991; Finkelstein *et al.*, 1998). Blood-lead levels of 60 μg/dL ($\sim$3 μM) or more can cause acute symptoms such as colic, headache, cramps, muscle weakness, depression, coma, and death (Johnson, 1998). The diverse effects of lead on a range of bodily systems suggests that lead affects the normal activity of numerous proteins.

In an attempt to understand the clinical effects of lead poisoning, the cellular and molecular effects of lead have been studied during the past few decades. Lead primarily acts by competing with endogenous cations on protein binding sites. In particular, lead can substitute for both calcium and zinc in numerous proteins (Goering, 1993; Goldstein, 1993; Simons, 1993; Zawia *et al.*, 1998). This substitution can further alter the normal functioning of these proteins and thus can alter cellular pathways and induce aberrant gene transcription (Zhu and Thiele, 1996; Bouton and Pevsner, 2000b). Examples of the alteration of the binding characteristics of the calcium-binding proteins include protein kinase C (PKC; Markovac and Goldstein, 1988; Goldstein, 1993; Bressler *et al.*, 1999), synaptotagmin I (Bouton *et al.*, 2001), and calmodulin (Habermann *et al.*, 1983; Goldstein and Ar, 1983; Fullmer *et al.*, 1985; Sandhir and Gill, 1994a,b,c; Ouyang and Vogel, 1998). Low nanomolar concentrations of lead can induce phospholipid binding of the synaptic vesicle protein synaptotagmin I and inhibit the binding of synaptotagmin I to its binding partner

[1] To whom correspondence should be addressed at Department of Neurology, Kennedy Krieger Institute, 707 N. Broadway, Baltimore, MD 21205. Fax: (410) 502-9083; E-mail: pevsner@kennedykrieger.org.

0041-008X/01 $35.00

syntaxin (Bouton *et al.,* 2001). These alterations in the binding characteristics of synaptotagmin I by lead may partially account for the effects of lead on neurotransmitter release (Manalis *et al.,* 1984).

Previous studies have demonstrated that the expression of numerous genes can be altered by lead (Bouton *et al.,* 2000b). The rat septohippocampal cholinergic system displays a selective sensitivity to lead poisoning that may be due in part to alterations in the transcriptional regulation and enzymatic activity of choline acetyltransferase (ChAT; Bielarczyk *et al.,* 1994, 1996; Tian *et al.,* 1996, 2000). Differential regulation of mRNA expression of the *N*-methyl D-aspartate (NMDA) subunit genes has also been observed following lead-exposure (Guilarte, 1997). In some cases, the alteration of the activity of some calcium-binding proteins by lead may lead to feedback regulation of the transcription of the mRNA transcripts corresponding to those genes. Alternatively, the perturbation of the activity of PKC by lead can cause altered transcriptional regulation of numerous mRNA transcripts that are regulated by PKC. Examples include fos and jun (Janknecht *et al.,* 1995; Foletta, 1996; Pennypacker *et al.,* 1997; Kim *et al.,* 1997, 2000; Chakraborti *et al.,* 1999), sialyltransferase (Davey and Breen, 1998), glial fibrillary acidic protein (GFAP) (Stoltenburg *et al.,* 1996; Zawia and Harry, 1996; Harry *et al.,* 1996), glutathione *S*-transferase P (GST-P) (Suzuki *et al.,* 1996), vascular endothelial growth factor (VEGF) (Hossain *et al.,* 2000), and neuromodulin (Schmitt *et al.,* 1996; Zawia and Harry, 1996; Harry *et al.,* 1996; Pennypacker *et al.,* 1997). The aberrant transcriptional activation of numerous mRNA transcripts can also be caused by the binding of lead to zinc-finger nucleotide binding proteins (Berg, 1990; Zawia and Harry, 1996; Berg and Godwin, 1997; Zawia *et al.,* 1998; Hanas *et al.,* 1999; Payne *et al.,* 1999). Finally, lead can alter the activity of zinc-dependent enzymes such as aminolevulinic acid dehydratase (Rocha *et al.,* 1995; Bergdahl *et al.,* 1997; Warren *et al.,* 1998) and carbonic anhydrase (Goering, 1993; Choi and Koh, 1998).

Considering the broad effects of lead, we hypothesized that large-scale gene expression profiling might lead to the identification of novel gene expression patterns perturbed by lead. Identification of these patterns would provide a large-scale view of the perturbation of cellular systems by acute lead poisoning and suggest certain proteins as putative novel molecular targets of lead poisoning. Therefore, we employed two different but complementary types of cDNA microarrays to detect differential gene expression in astrocyte cell cultures when treated with 10 μM lead for 24 h. Astrocytes, along with endothelial cells, comprise the blood–brain barrier. Lead is known to increase the permeability of the blood–brain barrier and can inhibit *in vitro* astrocyte–endothelial interactions relevant to brain microvessel development (Laterra *et al.,* 1992). These effects may contribute to the encephalopathy seen at a clinical level following high-level lead exposure, especially in children (Clasen *et al.,* 1973; Goldstein *et al.,* 1974; Press, 1977). Therefore, astrocytes are an important cellular target of lead (Tiffany-Castiglioni, 1993).

We recently reported that VEGF was one of the most differentially regulated genes identified in a cDNA microarray study of lead-exposed astrocytes (Hossain *et al.,* 2000). VEGF is an angiogenesis regulator that functions in the response of the blood–brain barrier to numerous types of insult (Ferrara and Henzel, 1989; Leung *et al.,* 1989; Bartholdi *et al.,* 1997; Cheng *et al.,* 1997). The lead-induced up-regulation of VEGF initially identified by microarray analysis was confirmed at the RNA level by Northern blotting and at the protein level by Western blotting. Further experimentation demonstrated a requirement for PKC-ϵ activation for the up-regulation of VEGF by lead. During these studies we conducted extensive tests to determine both an optimal concentration range and effective time course for the treatment of the astrocytes cell cultures with lead to determine the 10 μM lead concentration and 24-h time course used in the experiments reported herein.

In the present study we have confirmed as proof of principle the differential regulation of many genes previously reported to be affected by lead. These genes include VEGF, as described above, GFAP, and HSP70. In addition, we have identified the differential expression of numerous novel putative targets of acute lead treatment. We have applied the independent methods of RT–PCR and Western blotting in order to confirm the differential regulation of certain genes and proteins. We have used two complementary clustering methods to distinguish between lead-treated and two types of control-treated astrocytes solely based upon gene expression patterns detected in our microarray data. Additionally, we have employed bioinformatic methods in order to identify the coordinate regulation of groups of functionally related genes. Finally, based on our microarray results, we hypothesized that a specific protein, annexin A5, may be a molecular target of lead. We tested that hypothesis and demonstrated a direct effect of nanomolar concentrations of lead on the phospholipid binding characteristics of the annexin A5 protein.

MATERIALS AND METHODS

Clontech cDNA microarrays. Immortalized rat astrocytes, grown in 10-cm culture dishes to 80–90% confluency, were exposed to either 10 μM lead acetate (lead), 10 μM sodium acetate (sodium), or no treatment (control) for 24 h. Microscopic analysis of the cells before and after treatment was conducted. There was no discernable difference in the morphology or cell number between the lead versus control or sodium-treated astrocytes (data not shown), suggesting that the lead treatment did not cause nonspecific cytotoxicity. Furthermore, previous studies have demonstrated that astrocytes can withstand exposure to lead concentrations similar to those used here (Tiffany-Castiglioni, 1993) without detrimental affects to their viability. Total cellular RNA was extracted from the cells following treatment using RNeasy isolation kit (Qiagen) according to the manufacturer's protocol. Poly(A^+) RNA was isolated from total cellular RNA samples, reverse transcribed in the presence of [^{32}P]dATP to generate radiolabeled cDNA probe, and purified using Chromaspin-200 DEPC H_2O column chromatography according to the Atlas Pure RNA labeling protocol (Clontech). Clontech Neuroarray microarrays, repre-

senting 588 human neuron- and astrocyte-related genes, were hybridized with ^{32}P-labeled cDNA probes according to the manufacturer's instructions. The blots were exposed to a phosphorimaging screen at room temperature overnight and were visualized by phosphorimaging using Bio-Image analyzer BAS 2500 (Fujifilm).

Hybridized dot intensities on the microarrays were quantified using Clontech AtlasImage software. Normalization of the Clontech data was performed by subtracting the global background value of each microarray (calculated by AtlasImage) from the intensity value for each gene and then dividing the background-subtracted intensity value for each gene by the average intensity of all of the genes on that microarray. Average normalized intensity values were calculated for all genes derived from each microarray. Ratio values were calculated by dividing the average normalized intensity value for a given gene from one condition (e.g., lead) by the average normalized intensity value of that same gene from a different condition (e.g., sodium). Positive and negative signs were arbitrarily assigned to the ratio expression values (i.e., positive equals up-regulated in lead versus sodium and negative equals down-regulated in lead versus sodium). Two-tailed Student's *t* test *p* values were calculated for each gene by comparing the normalized intensity values derived from the four lead-treated cell samples against the normalized intensity values derived from either the four control-treated (*t* test PvC), the three sodium-treated cell samples (*t* test PvN), or the seven control and sodium samples combined (*t* test PvAll). Significantly differentially regulated genes were defined as those genes that had a normalized ratio intensity value of $\geq$1.8, a Student's *t* test PvAll *p* value of $<$0.05, and a Student's *t* test PvC or PvN (or both) *p* value of $<$0.05. Table 1 was compiled by integrating those genes that met these strict significance criteria across both the lead versus control and lead versus sodium measurements.

Incyte cDNA microarrays. cDNA for two Incyte UniGEM V microarrays, representing 9182 human genes with a wide variety of functions, was prepared from RNA samples. The RNA samples were derived from four independent preparations per condition of lead, sodium, or control astrocyte cultures yielding two pools of lead-exposed total RNA, one pool of sodium treated total RNA, and one pool of nontreated total RNA. Poly(A^+) RNA was purified from the total RNA pools with the Oligotex kit (Qiagen) and quantified with the RiboGreen RNA Quantitation kit (Molecular Probes) according to the manufacturer's instructions. The four Poly(A^+) RNA samples were sent to Incyte for further processing and hybridization to two UniGEM V microarrays. Data for the two Incyte microarrays were analyzed using Incyte GEMtools software.

Incyte provides intensity values for both the Cy3 (P1) and Cy5 (Balanced P2) signals derived from a microarray. A "balanced ratio expression" value is also provided in which, in a manner similar to the Clontech ratio expression values, up-regulation in one condition versus another condition is arbitrarily given a positive sign and down-regulation of that condition versus the other condition is arbitrarily given a negative sign. As in the Clontech data, in the Incyte data a positive value means up-regulation in lead-exposed samples and a negative value means down-regulation. A significantly, differentially regulated gene on the Incyte microarrays was defined as any gene having an absolute ratio expression value of $\geq$1.8. This cutoff was based upon extensive quality control experiments performed by Incyte (http://www.incyte.com/reagents/gem/GEM_Validation.pdf).

In order to analyze the coordinated regulation of gene families the set of 17,678 gene ratio expression values derived from both of the Incyte microarrays was cross-referenced with the entire SWISS-PROT database (http://expasy.proteome.org.au/sprot/) using the DRAGON database (Bouton and Pevsner, 2000a) to annotate the gene expression set with SWISS-PROT keywords. The resulting annotated data set was visualized using the DRAGON Families tool (Bouton and Pevsner, submitted for publication http://pevsnerlab.kennedykrieger.org/dragon.htm). To further investigate the two families that were identified in the DRAGON Families analysis, the set of 17,678 gene ratio expression values was integrated with all possible "default hierarchy nodes" provided by Incyte GEMtools software. The distributions of gene expression values present in each of the resulting subsets of genes were compared against the distribution of all 17,678 gene expression values using a χ^2 analysis in Microsoft Excel. A set of strict criteria was employed to identify significantly differentially regulated gene families. A significant family (1) had to have at least 20 gene expression measurements; (2) at least 3 of those measurements had to have an absolute value of $\geq$1.8; (3) at least 10 of those measurements had to be in the same direction; and (4) the family had to have a χ^2 *p* value of less than 0.0001 as compared to the distribution of all 17,678 gene measurements.

RT–PCR. Primers used were as follows: Chloride channel 3 (CLC3): forward, 5′-GCA TTT ATG AAG CAC ACA TCC-3′ reverse, 5′-GTT TGC CGT CTG GGC CAT ATG-3′; phospholipase A2 (PLA2): forward, 5′-GCT CTA GAG CCA CCA TGC AGC ACA TAA TAG TGG AAC AC-3′ reverse, 5′-CCC CCC GGG TCA CTC TCC CAC CTT CAT AGA AGA-3′; glyceraldehyde-3-phosphate dehydrogenase (GAPDH): forward, 5′-ACC ACC ATG GAG AAG GCT GG-3′ reverse, 5′-CTC AGT GTA GCC CAG GAT GC-3′; annexin 5: proprietary Clontech primer, sequence unavailable; and creatine transporter 1 (CT1): proprietary Clontech primer, sequence unavailable.

cDNA was generated from the same 12 RNA samples used on both the Clontech and Incyte microarrays using the SuperScript II Reverse Transcriptase kit (Life Technologies). A Lightcycler PCR thermo-cycler (Roche) was used to perform PCR reactions in order to monitor the linear range of gene product amplification in real-time. Reactions were stopped while amplification of the gene product was in the linear range and a melting temperature for each product was calculated in order to determine specificity of the PCR reaction (data not shown). PCR gene products were electrophoresed on agarose gels and quantitated using Scion Image software (www.scion.com). Band intensities measured for each gene product were normalized by dividing each intensity value by the intensity value of a corresponding GAPDH band amplified from the same cDNA sample.

Western blotting. Rat astrocytes were grown to 80–90% confluency in 10-cm petri dishes and the cytosolic fraction of Dounce homogenates was collected by differential centrifugation as previously described (Bouton *et al.*, 2001). These cells were independent of those used in the preparation of RNA for microarray hybridization and RT–PCR reactions. Briefly, cells were detergent-solubilized in Buffer A (50 mM Hepes, 150 mM NaCl, pH 7.4) containing 0.5% Triton X-100. The nuclear fraction was separated by centrifugation at 10,000*g* for 15 min. The supernatant was centrifuged at 100,000*g* for 20 min in order to isolate the cytosolic fraction. Equivalent amounts of cytosolic fraction were loaded on 10% SDS–PAGE, electrophoresed, and transferred to nitrocellulose. Ponceau S staining of the blots confirmed proper transfer and equal loading of protein lanes. Antibodies specific for annexin 1 (Transduction Laboratories), annexin 5 (StressGen), MARCKS (Upstate Biotechnology), and syntaxin 1 (Sigma) were incubated with replicate nitrocellulose blots overnight at 4°C. The blots were washed three times, 10 min each in PBS-T and incubated with appropriate peroxidase-conjugated secondary antibody. Three 10-min washes in PBS-T were followed by incubation in ECL (Amersham Pharmacia) and exposure to radiographic film (Kodak X-OMAT AR). Protein band intensities were quantitated using Scion Image software. Band intensities were normalized by dividing each specific intensity value by corresponding intensity values measured from a nonspecific band present across all blots and localized to each gel lane as visualized by Ponceau S staining (data not shown).

Annexin A5/phospholipid binding assay. A his6-tagged fusion in the pET22b prokaryotic expression vector containing the entire open reading frame of annexin A5 was obtained from the laboratory of Dr. Mark Schlissel. The annexin A5 open reading frame was amplified from the pET22b construct using PCR primers with sequences 5′-TCG CCA TGG CAC AGG TTC TCA G-3′ and 5′-CGC AAG CTT GTC ATC TTC TCC ACA GAG-3′. The resulting PCR product was cloned into the pGEX-KG expression vector using *Hin*dIII and *Nco*I restriction enzymes. The resulting plasmid construct was heat-shock transformed into DH10B *Escherichia coli* bacteria. Preparation of recombinant GST-tagged annexin A5 protein was by growth and lysis of the *E. coli* bacteria followed by precipitation with glutathione sepharose beads (Pharmacia). Thrombin cleavage for 1 h at room temperature was used to dissociate the protein from its GST tag. SDS–PAGE and Coomassie blue staining were used to confirm the size, purity, and concentration of the protein (Fig. 8A).

Tritiated phospholipid liposomes composed of lipid bilayers were prepared as previously described (Davletov and Südhof, 1993; Chapman and Jahn, 1994; Bouton *et al.,* 2001). Briefly, brain phosphatidylserine (PS) (Avanti Polarlipids), brain phosphatidylcholine (PC) (Avanti Polarlipids), and [^{3}H]PC (Amersham) were stored in chloroform at −80°C. Glass capillary tubes were used for measurement of appropriate volumes of phospholipid. Seventy-five percent PC, 25% PS and approximately 0.1 mCi/ml of [^{3}H]PC were mixed and dried under a stream of nitrogen gas. The dried lipid mixture was resuspended in Buffer A and probe sonicated for 30 s. Centrifugation for 1 min at 5000*g* precipitated large phospholipid aggregates, yielding a supernatant containing a suspension of liposomes.

Phospholipid binding assays were performed as described (Davletov and Südhof, 1993; Chapman and Jahn, 1994; Bouton *et al.,* 2001). Chelator types and concentrations were calculated based on chelator-cation dissociation constants from Martell and Smith (1989) with the software program "Chelator" (Schoenmakers *et al.,* 1992). Chelators used were EGTA, nitrilotriacetic acid (NTA), and *N*-benzyliminodiacetic acid (*N*-BIDA). [^{3}H]Phospholipid liposomes, thrombin-cleaved recombinant annexin A5 protein, annexin A5 antibody (A. G. Scientific Inc.), Protein-G Sepharose (Pharmacia), and calculated concentrations of chelator and CaOAc or PbOAc were brought to a total volume of 100 μl with Buffer A. Reactions were incubated for 1 h at 4°C. Samples were washed three times in 500 μL per wash with incubation buffer and then resuspended in Ecolite scintillation fluid. Levels of radioactivity in each sample were determined by liquid scintillation spectroscopy. Curves were fit to the data with the equation $R = (R_{max} \times [M])/(EC50 + [M])$ as previously described by Tomsig and Suszkiw (1995). R_{max} is the maximum amount of phospholipid precipitated, $[M]$ is the concentration of metal, and EC50 is the concentration of metal at which binding is half-maximal. The amount of radioactive isotope in 10 μl of labeled phospholipid was measured for each experiment. All experiments were performed in triplicate. In order to normalize our data, background levels of radioactivity (amount of radioactivity precipitated by annexin A5 protein in the absence of cations) were subtracted from all measurements. The amount of radioactivity precipitated in each condition was then multiplied by 10,000 and divided by the total amount of radioactivity present in 10 μl of phospholipid liposomes.

RESULTS

Clontech Microarrays

Twelve Clontech Neuroarrays, representing 588 genes that encode proteins involved in neuronal and astrocytic processes, were hybridized with cDNA prepared from 12 independent samples derived from quadruplicate cell cultures treated with three different conditions: no treatment (control), 10 μM sodium acetate (sodium) as a control for acetate, or 10 μM lead acetate (lead). Data from one of the sodium blots were discarded due to the substandard quality of the blot hybridization, leaving data from 11 arrays (4 control replicates, 3 sodium replicates, and 4 lead replicates). Of the 588 genes represented on the Clontech Neuroarrays, 418 were detected according to predefined criteria (see Materials and Methods) on at least one array. This set of 418 genes was used for all further Clontech data analyses. Normalized expression values were calculated as described under Materials and Methods.

Scatter plots of the log average lead versus either log average control (Fig. 1A) or sodium (Fig. 1B) normalized intensity values indicated even distributions of gene intensity values between the lead and the two control data sets. Strict conditions were applied in order to identify those genes that were significantly differentially regulated among the 418 genes (Figs. 1A and 1B open circles). These conditions were, first, a ratio expression value of ≥1.8 (chosen due to its correspondence with the ratio expression value used with the Incyte data) and, second, a Student's *t* test value of $p < 0.05$ calculated across replicate measurements from each condition for every gene. Ninety-four of 418 genes (22%) met these criteria in the lead versus control data. Of those 94 genes, 80 were up-regulated (85%) and 14 were down-regulated (15%). Sixty of 418 genes (14%) met these criteria in the lead versus sodium data. Of those 60 genes, 48 were up-regulated (80%) and 12 were down-regulated (20%). Forty-four genes were shared across these two sets of genes (Table 1). Of those 44 genes, 36 were up-regulated (82%) and 8 were down-regulated (18%). Figure 2 displays the average normalized expression values and hybridized dots from the 11 microarrays for a representative set of 18 genes.

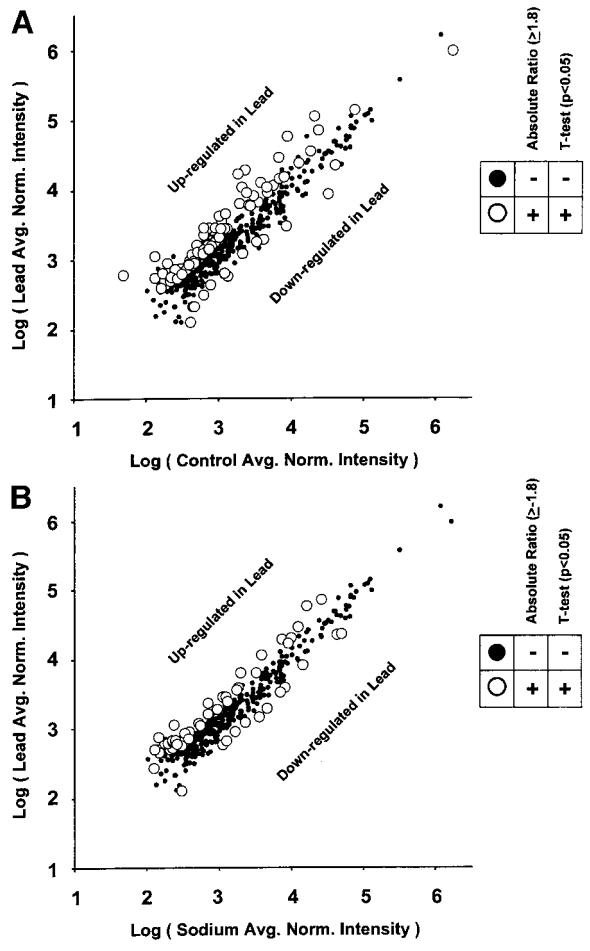

FIG. 1. Average intensity values were calculated from replicate microarrays hybridized with cDNA derived from astrocytes treated with three different conditions. Scatter plots of the log values of averages were plotted in two graphs, comparing lead- versus control-treated cells (A) and lead- versus sodium-treated cells (B). Significantly differentially regulated genes (open circles) were identified as those genes with both a ratio expression value ≥1.8 and a Student's *t* test value of $p < 0.05$ (see Materials and Methods).

TABLE 1

Forty-four Genes Significantly Differentially Regulated in Lead-Exposed Astrocytes as Determined by Clontech Microarray Analysis

Student's *t* tests[a]			Ratios[b]		Gene information[c]	
PvC	PvN	PvAll	PvC	PvN	Genbank	Gene name
1.9E-04	2.3E-03	2.1E-05	12.1	3.3	Z35309	Ca^{2+}/calmodulin-activated adenylyl cyclase
6.1E-05	1.3E-02	7.5E-04	8.7	1.8	M29870	p21-rac1
1.1E-03	8.3E-03	5.1E-05	8.3	4.6	J03746	Microsomal glutathione *S*-transferase 12
1.1E-03	3.1E-02	5.5E-04	8.0	2.5	U07550	Mitochondrial 10-kDa heat shock protein (HSP10)
2.5E-03	1.7E-02	1.8E-04	6.5	3.5	L15189	Heat shock protein 70 (HSP70)
4.0E-03	4.2E-02	9.8E-04	4.5	2.2	M31659	GT mitochondrial solute carrier protein homolog
2.6E-03	3.2E-02	5.9E-04	4.2	2.3	X54297	Histidine decarboxylase (HDC)
2.5E-03	6.0E-02	1.8E-03	4.0	1.9	M14780	Creatine kinase M subunit
1.2E-03	2.7E-03	7.6E-05	4.0	2.7	X68203	Vascular endothelial growth factor receptor 3 precursor
4.9E-04	6.5E-03	3.9E-05	3.8	2.5	M21054	Lung group IB phospholipase A2 precursor (PLA2)
3.3E-05	1.1E-02	1.6E-04	3.7	2.5	M34424	Lysosomal alpha-glucosidase precursor
1.6E-05	1.3E-04	6.4E-08	3.2	3.1	L18983	Protein-tyrosine phosphatase N precursor (PTP IA-2)
1.8E-03	2.9E-02	4.5E-04	3.1	2.0	X12454	Annexin V
3.5E-03	2.2E-02	3.4E-04	3.1	2.2	X78520	Chloride channel protein 3 (CLC-3)
1.1E-05	1.2E-04	3.3E-08	3.0	2.7	M32977	Vascular endothelial growth factor precursor (VEGF)
4.3E-03	6.0E-02	2.2E-03	2.8	2.0	D23672	Biotin-[methylmalonyl-CoA-carboxyltransferase] ligase
2.6E-02	1.1E-01	7.4E-03	2.6	2.0	L12387	Sorcin 22-kDa protein (SRI)
1.0E-02	1.3E-01	1.9E-02	2.5	1.9	U00803	Tyrosine-protein kinase FRK
4.4E-03	6.9E-04	2.0E-04	2.5	5.0	S70609	Sodium- and chloride-dependent glycine transporter 1
1.2E-02	1.8E-02	6.6E-04	2.5	3.2	U53476	WNT7A protein precursor
7.6E-06	3.2E-05	2.0E-07	2.4	2.9	M59371	Ephrin type-A receptor 2 precursor
1.6E-02	5.0E-02	2.1E-03	2.4	2.2	M22960	Cathepsin A; carboxypeptidase C
3.0E-02	1.0E-01	6.8E-03	2.4	1.9	L37792	Syntaxin 1A (STX1A)
1.3E-01	2.5E-02	3.1E-02	2.3	3.3	M88461	Neuropeptide Y receptor type 1 (NPY1R)
7.5E-03	3.0E-02	2.0E-03	2.3	2.0	X13227	D-amino acid oxidase (DAMOX; DAO; DAAO)
1.8E-02	1.1E-02	1.3E-03	2.2	3.3	M22430	Synovial group II phospholipase A2
4.0E-03	3.2E-02	7.0E-04	2.2	1.9	AF007548	Golgi SNARE; GS27
3.6E-02	9.4E-02	6.7E-03	2.2	1.9	M30773	Calcineurin B subunit isoform 1
7.8E-03	4.8E-03	3.4E-04	2.0	2.9	L31409	Na- and Cl-dependent creatine transporter 1 (CT1)
2.9E-02	2.6E-02	3.1E-03	2.0	2.5	L13943	Glycerol kinase (GK)
4.9E-04	3.5E-03	6.8E-05	2.0	2.4	X97867	Serine/threonine phosphatase
4.4E-02	6.6E-02	7.6E-03	1.9	2.1	X62535	Diacylglycerol kinase alpha (DAG kinase alpha)
1.5E-02	2.0E-02	1.2E-03	1.9	2.0	M58026	Calmodulin-related protein NB-1
9.9E-03	3.7E-03	6.4E-04	1.9	2.7	Z67743	Chloride channel protein 7 (CLC-7)
8.4E-04	1.2E-03	1.5E-05	1.9	2.2	M29273	Myelin-associated glycoprotein precursor (MAG)
5.8E-02	1.7E-02	5.8E-03	1.8	3.5	U00802	Drebrin E
3.7E-03	3.1E-03	4.4E-04	−1.8	−1.9	M68956	Myrist.alanine-rich C-kinase substrate (MARCKS)
2.6E-02	4.6E-03	3.7E-03	−1.8	−1.9	X79204	Ataxin-1
9.6E-04	1.1E-04	2.1E-05	−2.2	−2.5	M98529	Neuron-specific protein family member 1 (NSG1)
4.8E-04	4.4E-04	1.2E-04	−2.4	−2.0	X75208	Ephrin type-B receptor 3 precursor
2.4E-03	4.3E-04	1.2E-03	−3.3	−2.4	Z18956	Sodium- and chloride-dependent taurine transporter
4.3E-03	1.8E-01	2.8E-02	−3.8	−1.9	U60519	Caspase-10 precursor (CASP10)
1.2E-01	4.9E-02	3.6E-02	−4.2	−4.3	D10995	5-hydroxytryptamine 1B receptor (5-HT-1B)
3.7E-03	3.6E-01	3.5E-02	−7.1	−2.7	K02268	Beta-neoendorphin-dynorphin precursor

Note. Genes that were down-regulated in lead-treated astrocytes are displayed with their ratio expression values with a grey background; genes that were up-regulated in lead-treated astrocytes have ratio expression values with a white background.

[a] The two-tailed Student's *t* test *p* value for the comparison of replicate samples values for each gene between either lead and control (PvC), lead and sodium (PvN), or lead versus both the control and sodium values (PvAll).

[b] The ratio expression values for the average expression values of each gene between lead and control (PvC) or lead and sodium (PvN).

[c] The Genbank accession numbers and gene names for each gene.

Various clustering techniques have been employed extensively in the analysis of microarray data in order to identify similarities in gene expression patterns across entire data sets. We clustered the Clontech data using two complementary methods to test whether the gene expression pattern caused by lead treatment was distinguishable from control or sodium treatment. The data for the 418 detected genes were imported into both the Cluster/Treeview (http://rana.lbl.gov/EisenSoftware.htm) and Partek (www.partek.

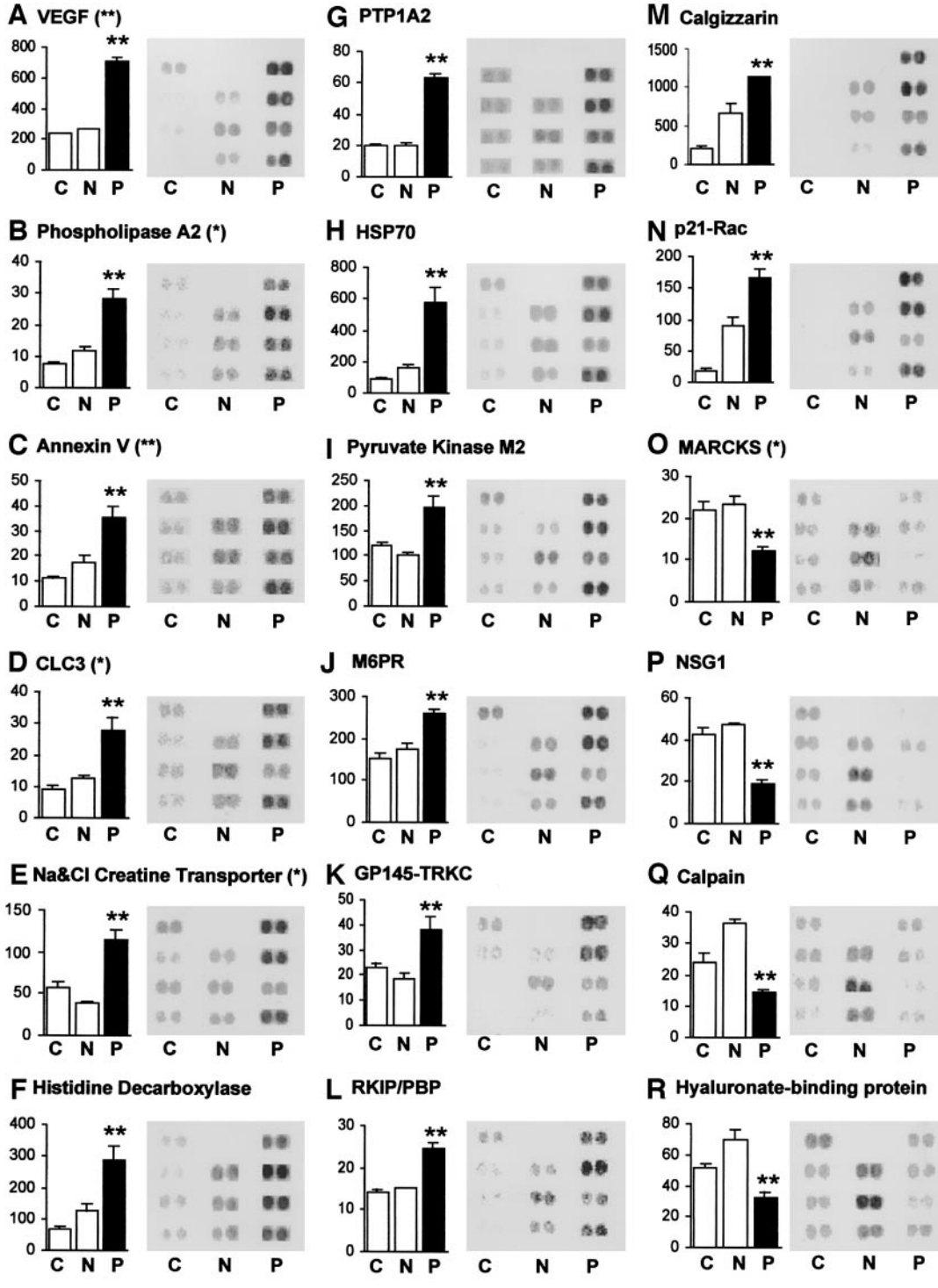

FIG. 2. Representative set of dots derived from the Clontech microarrays. Each panel contains a gene name, a bar graph representing the intensity values for that gene across 11 microarrays, and pictures of the actual dots representing that gene from each of the 11 microarrays. *Confirmation of differential regulation of that gene by RT–PCR or Northern or Western blotting. **Confirmation by more than one method. Error bars represent standard deviation.

com) analysis software packages for clustering analysis. Using Cluster/Treeview (Eisen *et al.*, 1998; Chu *et al.*, 1998; Alizadeh *et al.*, 2000), a hierarchical clustering tree of the normalized intensity values for each of the 11 microarrays was generated. All four of the lead-treated data sets were clustered away from both the sodium and control data sets. As expected, there was not a clear distinction between the control and sodium data sets (Fig. 3A). As a complementary form of analysis, the Clontech data were im-

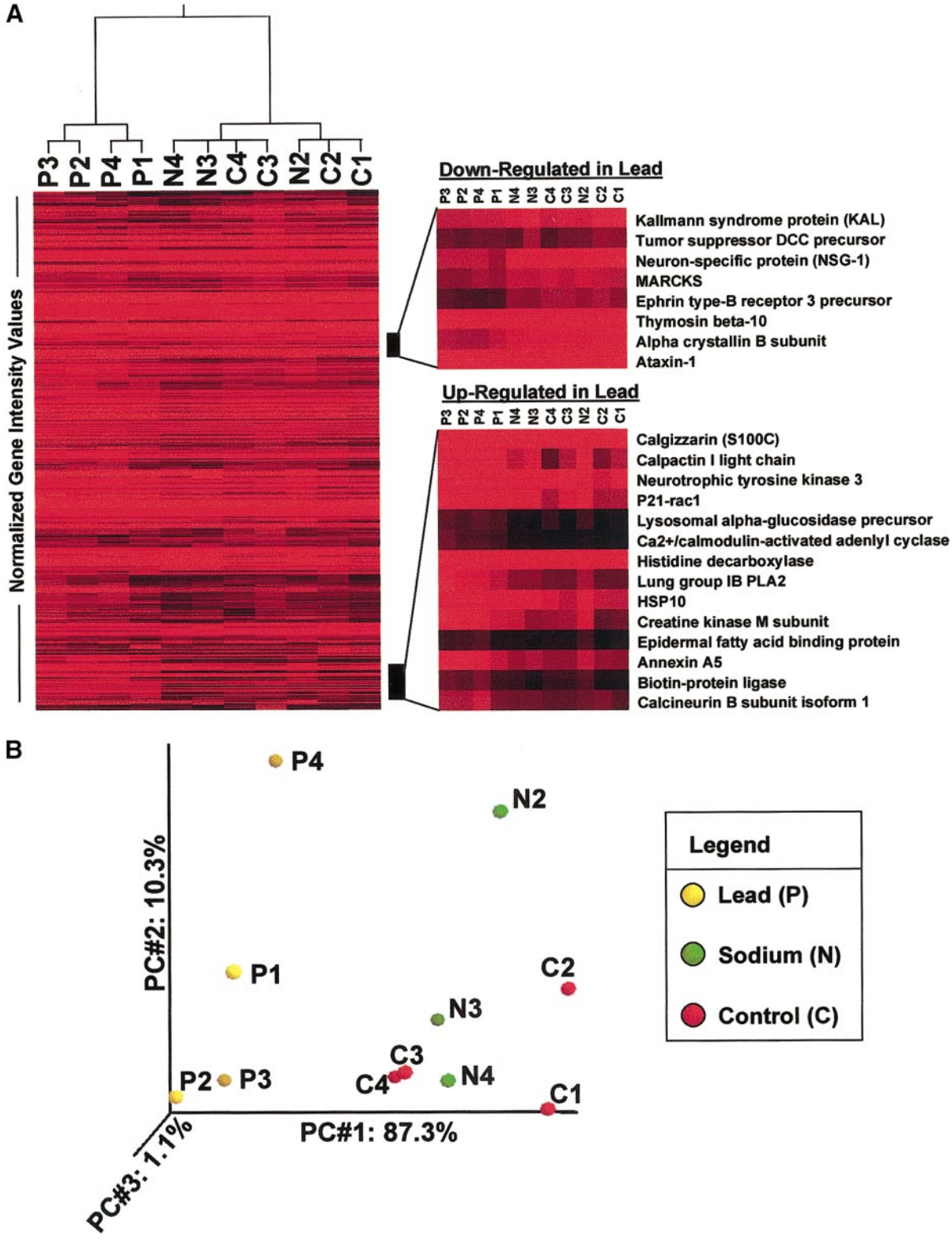

FIG. 3. (A) The intensity values of 418 genes from 11 Clontech microarrays (C1–4, N2–4, and P1–4 were clustered using a centered hierarchical clustering algorithm in Cluster. Treeview was used to visualize the clustered data. (B) Principal components analysis (PCA) of the 11 Clontech microarray data sets. Each dot represents all of the data (418 genes) derived from one microarray. The color of each dot (yellow, lead; green, sodium; and red, control) represents the treatment condition for the sample applied to that microarray.

ported into the Partek data analysis software package and clustered using principal components analysis (PCA). Proximity in PCA space is indicative of similarity of gene expression patterns between microarray data sets (Gnanadesikan, 1977). In a manner similar to the hierarchical clustering method, the four lead samples were separated from both the control and the sodium samples across the first principal component, which accounted for 87.3% of the variance in the data (Fig. 3B). Furthermore, the control and sodium representations in PCA space were intermixed, indicating less difference between them.

Incyte Microarrays

We obtained additional gene expression data using Incyte UniGEM V microarrays. These microarrays contain genes with a wide range of cellular functions. The expression of 9182 genes was analyzed on two fluorescence-based microarrays using pooled cDNA samples derived from the same RNA as that used on the Clontech Neuroarrays. On one array a pooled control-treated cDNA sample was compared against a pooled lead-exposed cDNA sample (PvC). On the other array a pooled sodium-treated cDNA sample was compared against a replicate, pooled lead-exposed cDNA sample (PvN). Scatter plots for the log intensity values derived from the PvC (Fig. 4A) and PvN (Fig. 4B) data sets provide a graphical representation of significantly differentially regulated genes in the two data sets. The "balanced differential expression" value (hereafter referred to as a "ratio expression value") provided by Incyte was used as the measure of differential regulation for each gene. An absolute ratio expression value cutoff of $\geq$1.8 was set (see Materials and Methods). On the PvC array, 77 of 8927 genes (0.9%) had an absolute ratio expression value of $\geq$1.8. Of those 77 genes, 48 were up-regulated (62%) and 29 were down-regulated (38%). On the PvN array, 179 of 8751 genes (2%) had an absolute ratio expression value of $\geq$1.8. Of those 179 genes, 113 were up-regulated (63%) and 66 were down-regulated (37%). Presumably the lower percentage of significantly differentially regulated genes on the Incyte arrays as compared to the Clontech Neuroarrays was due to the fact that the Incyte arrays are not specific to neuronal and astrocytic genes. Fifty-two genes (0.3% of all genes) were common between the two Incyte data sets (Table 2). Of those 52 genes, 34 were up-regulated (65%) and 18 were down-regulated (35%). Of the 418 genes in the Clontech data set, 282 were also represented on the Incyte microarrays. Of these 282 genes, ~80% were expressed in the same direction across the Clontech and Incyte microarrays, indicating substantial correlation between the two data sets. Of these, the most significantly different genes shared across both Clontech and Incyte arrays were neuron specific gene 1 (NSG1), heat shock protein 70 (HSP70), chloride channel 3 (CLC3), and lumican.

In an attempt to identify the coordinate regulation of functionally related gene groups, we used two complementary methods. The coordinate regulation of groups of functionally related genes

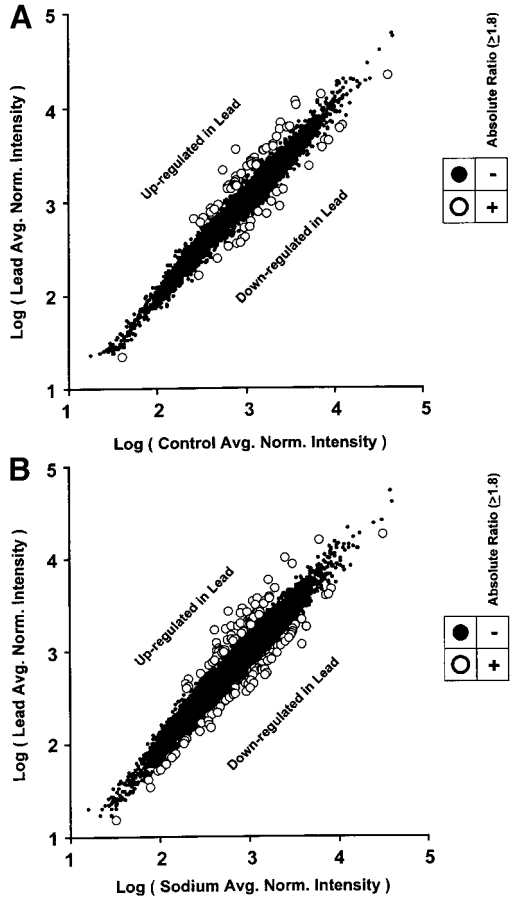

FIG. 4. Scatter plots of the log values of fluorescent intensity values derived from Incyte microarrays were plotted in two graphs, one comparing lead- versus control-treated cells (A) and another comparing lead- versus sodium-treated cells (B). Significantly differentially regulated genes (open circles) were identified as those genes with a ratio expression value $\geq$1.8 (see Materials and Methods).

has been identified in numerous studies (Wen *et al.*, 1998; Chu *et al.*, 1998; Eisen *et al.*, 1998; Spellman *et al.*, 1998; Heyer *et al.*, 1999; Mirnics *et al.*, 2000). Often, the identification of such groups can provide insight into the types of cellular processes that have been perturbed in the experimental state. We first employed the DRAGON database (Bouton and Pevsner, 2000a) and its associated information visualization tools known as DRAGON View (http://pevsnerlab.kennedykrieger.org/dragonview.htm) to screen our entire Incyte data set for the coordinate regulation of functionally related genes. The two Incyte data sets, comprising 17,678 genes, were combined and annotated with SWISS-PROT database keywords using the DRAGON Database. Using the SWISS-PROT keywords, the DRAGON View analysis indicated that the tRNA synthetase and collagen families were the two largest coregulated gene groups in the entire combined data set (Fig. 5A). In order to determine the significance of the altered expression of these two groups, we employed the default hierarchy nodes provided by GEMtools in a manner similar to that

TABLE 2
Fifty-two Genes Significantly Differentially Regulated in Lead-Exposed Astrocytes as Determined by Incyte Microarray Analysis

Ratios and intensity values[a]						Gene information[b]	
PvC			PvN				
PvC	P1	B-P2	PvN	P1	B-P2	Genbank	Gene name
4.5	777	3534	4.5	586	2660	AC005326	Asparagine synthetase
3.9	552	2130	4	415	1669	AJ252550	Glycerol kinase
3.1	3656	11411	4	2512	9960	L11066	Heat shock 70 kDa (HSP70)
2.8	3766	10436	2.7	3101	8448	L11066	Heat shock 70 kDa (HSP70)
2.7	2477	6692	2.4	1967	4675	NM_005412	Serine hydroxymethyltransferase 2 (mitochondrial)
2.4	767	1822	3.1	802	2500	NM_004539	Asparaginyl-tRNA synthetase
2.4	1131	2670	3.1	1094	3388	NM_006636	Methylene tetrahydrofolate dehydrogenase
2.3	620	1397	2.3	431	975	Z14136	Spermidine/spermine *N*1-acetyltransferase
2.3	1030	2359	2.4	751	1806	AW070645	RNB6
2.3	1270	2858	2.7	950	2578	BE299937	Methionine-tRNA synthetase
2.2	630	1355	1.9	401	764	AI970531	Branched chain aminotransferase 1
2.2	1550	3432	2.3	1488	3410	U89436	Tyrosyl-tRNA synthetase
2.2	1172	2618	2.9	1239	3600	NM_004446	Glutamyl-prolyl-tRNA synthetase
2.2	653	1463	3.1	547	1688	X59892	Tryptophanyl-tRNA synthetase
2.2	1146	2552	3.3	848	2838	NM_001550	Interferon-related developmental regulator 1
2.1	1738	3597	1.8	1277	2257	AA598841	Natriuretic peptide receptor A/guanylate cyclase A
2.1	779	1650	2.2	583	1300	AW372543	Activating transcription factor 6
2.1	1168	2432	2.4	816	1951	AL078459	Dimethylarginine dimethylaminohydrolase 1
2.1	1613	3452	2.6	1190	3081	AA477660	Eukaryotic translation initiation factor 3, subunit 8 (110 kDa)
2.1	906	1939	2.9	628	1839	Z31713	Solute carrier family 1 (glial high affinity glutamate transporter)
2.1	2250	4745	3.5	1648	5723	U72508	B7 protein
2	724	1480	1.8	524	950	M63180	Threonyl-tRNA synthetase
2	407	831	2	289	567	—	Incyte EST {Incyte PD:4327691}
2	1314	2566	2.1	986	2077	NM_002940	ATP-binding cassette, subfamily E (OABP)
2	680	1354	2.1	453	962	Z15005	Centromere protein E (312 kDa)
2	336	657	2.2	199	436	NM_007235	Exportin, tRNA (nuclear export receptor for tRNAs)
1.9	310	589	1.8	189	333	L29008	Sorbitol dehydrogenase
1.9	776	1454	1.9	415	773	AB018274	KIAA0731 protein
1.9	443	821	2.3	213	490	NM_005308	G protein-coupled receptor kinase 5
1.9	7169	13428	2.6	6064	15472	BE301211	Ferritin, light polypeptide
1.9	494	920	2.8	430	1213	NM_001693	ATPase, H^+ transporting, lysosomal (vacuolar proton pump)
1.8	1210	2131	2	998	2018	AI752707	Glutathione *S*-transferase like
1.8	1527	2697	2.1	1038	2165	AL036415	Low molecular mass ubiquinone-binding protein (9.5 kDa)
1.8	1313	2373	2.1	1201	2539	X95073	Translin-associated factor X
−1.8	607	345	−2.3	359	159	M64110	Caldesmon 1
−1.8	2239	1243	−1.9	1639	867	U09559	Karyopherin alpha 2 (RAG cohort 1, importin alpha 1)
−1.9	963	517	−1.9	657	342	NM_001046	Solute carrier family 12 (sodium/potassium/chloride transporters)
−2	2634	1305	−2.8	1574	562	L27560	Human insulin-like growth factor binding protein 5 (IGFBP5)
−2	634	325	−2.7	1025	386	AA975473	Neuron-specific protein 1
−2	7402	3677	−2	7877	3955	AI929630	ESTs
−2	484	240	−2	353	173	NM_003247	Thrombospondin 2
−2	8764	4342	−1.9	7237	3908	M63473	Collagen, type IV, alpha 5 (Alport syndrome)
−2	1934	976	−1.9	1540	832	X78565	Hexabrachion (tenascin C, cytotactin)
−2	40973	20984	−1.8	32123	17855	AW410427	Collagen, type II, alpha 1 (primary osteoarthritis, congenital)
−2.1	1124	528	−2	1098	537	AI878826	Caveolin 1, caveolae protein, 22 kDa
−2.2	5193	2340	−3.4	3936	1142	AW157548	Insulin-like growth factor binding protein 5
−2.3	795	352	−2.4	1493	612	N85304	Annexin A1
−2.4	1723	731	−2.8	1488	531	NM_004772	P311 protein
−2.4	867	355	−2.6	1132	441	NM_001797	Cadherin 11
−2.4	979	408	−2.3	1061	465	NM_004791	Integrin, beta-like 1 (with EGF-like repeat domains)
−2.4	923	389	−2.1	915	434	NM_016447	MAGUK protein p55T
−2.8	2423	880	−2.2	1784	797	AL036211	Lumican

Note. Genes that were down-regulated in lead-treated astrocytes are displayed with their ratio expression values with a grey background; genes that were up-regulated in lead-treated astrocytes have ratio expression values with a white background.

[a] The ratio expression values for the average expression values of each gene between lead and control (PvC) or lead and sodium (PvN).

[b] The Genbank accession numbers and gene names for each gene.

previously described (Mirnics *et al.,* 2000). GEMtools provided two functional classifications (tRNA charging, Table 3A and Collagens, Table 3B) that closely matched the same gene groups identified with SWISS-PROT keywords.

χ^2 analysis was used to determine the statistical significance of the compared distribution histograms of all genes on the two Incyte arrays against the distribution histograms of the tRNA charging and collagens groups. Both groups were calculated to have expression profiles that were significantly different from that of the combined data set (Fig. 5B) according to the strict criteria of $p < 0.0001$ (see Materials and Methods). Of the 250 GEMtools functional gene groups analyzed, the Amino Acid Biosynthesis gene group was the only other gene group that also displayed coordinated differential regulation according to χ^2 analysis (Fig. 5B and Table 3C). When the PvC and PvN data sets are examined independently, the tRNA synthetase and collagen families have similar coordinate expression in each (Table 3). The altered distribution of the tRNA synthetase and collagen families is not accounted for by the size of the family. Many other gene families of similar size such as the actins and neuropeptides (Fig. 5B) have distributions that are not significantly different than the distribution of all genes. We tested the distribution of three other gene groups that we hypothesized might be coordinately regulated according to previous observations regarding the perturbation of gene expression patterns caused by lead. These groups were calcium transporters/channels (Calcium Transporters), Metalloproteases, and Zinc-binding transcription factors (Fig. 5B). None of these groups demonstrated coordinated differential regulation.

Differential Gene Expression Confirmations

In order to independently confirm the results obtained from our microarray analysis, we conducted RT–PCR and Western blotting analysis of a randomly selected subset of differentially regulated genes identified by microarray analysis. These experiments were intended to demonstrate that the differential regulation of selected subsets of genes could be confirmed by independent methods. Therefore, the genes were randomly selected so as not to bias our confirmations toward genes that were previously known to be differentially regulated by lead. RT–PCR analysis performed on quadruplicate samples from each of the three different conditions confirmed the differential regulation of four genes: cytosolic phospholipase A2 (PLA2; Fig. 6A), annexin A5 (Fig. 6B), chloride channel 3 (CLC3; Fig. 6C), and creatine transporter 1 (CT1; Fig. 6D) compared to the consistent expression of GAPDH (Fig. 6E) across all 12 samples. Western blotting performed in duplicate on independently prepared cytosolic fractions of astrocyte cell cultures confirmed the differential regulation of four different gene products. The microarray analysis corresponded with an altered level of the corresponding encoded proteins. These genes were annexin A5 (Fig. 7A), syntaxin (Fig. 7B), annexin A1 (Fig. 7C), and myristolated alanine-rich C kinase substrate (MARCKS, Fig. 7D).

Annexin A5 Phospholipid Binding Assay

The differential regulation of annexin A5 by lead was detected on the Clontech microarrays (Fig. 2C and Table 1). Annexin A5 is not present on the Incyte UniGEM V microarray; however, three other annexins, A1, A4, and A7, are all on the UniGEM V microarray. Of these, annexin A1 was significantly differentially regulated on both the PvC and PvN microarrays (Table 2) and confirmed by Western blotting (Fig. 7C). The annexins are a family of calcium-dependent, phospholipid binding proteins involved in signal transduction and other cellular processes. These characteristics suggested that the annexins may be direct molecular targets of lead via substitution for calcium in their cation binding domains. Specifically, we hypothesized that lead promotes annexin A5 binding to phospholipid in a manner similar to its effects on the phospholipid binding characteristics of both PKC and synaptotagmin I. Therefore, we chose to study the effects of lead on annexin A5 more extensively. We first confirmed the differential regulation of annexin A5 mRNA by RT–PCR (Fig. 6B) and annexin A5 protein by Western blotting (Fig. 7A). We then isolated pure recombinant human annexin A5 as a thrombin-cleaved GST fusion protein (Fig. 8A) for use in tritiated 75% phosphatidylcholine/25% phosphatidylserine phospholipid liposome binding assays. In the absence of annexin A5, phospholipid liposomes are not precipitated under any condition. However, upon the addition of annexin A5, significant amounts of phospholipid liposomes were precipitated in the presence of 200 μM Ca^{2+} and 10 nM Pb^{2+} (Fig. 8B). The binding affinity of annexin A5 to phospholipid liposomes was determined across a physiologically relevant concentration range of lead (Fig. 8C). Statistically significant binding effects were observed at lead concentrations as low as ~8 nM. A half-maximal binding concentration of ~30 nM lead was observed for the binding of annexin A5 to phospholipid liposomes, with a saturating concentration of ~100 nM.

DISCUSSION

Clustering Methods

A central tenet in the field of toxicogenomics is that specific toxicant "signatures" can be detected through the use of large-scale genome-based technologies such as microarrays (Nuwaysir *et al.,* 1999). These signatures consist of the observation of genome-wide patterns of gene expression in response to treatment of a specific cell or tissue type with a toxicant (Afshari *et al.,* 1999; Rockett and Dix, 1999). One aim of signature identification is the classification of known toxicants into categories based upon specific gene expression patterns in specific tissue types. This library of signatures could then be used to rapidly and inexpensively screen novel drug candidates (Marton *et al.,* 1998; Wilson *et al.,* 1999) or suspected toxicants for similarities to known toxicants. To date, a few studies have demonstrated the ability to identify toxicant signatures through microarray analysis (Gasch *et al.,* 2000; Burczynski *et al.,*

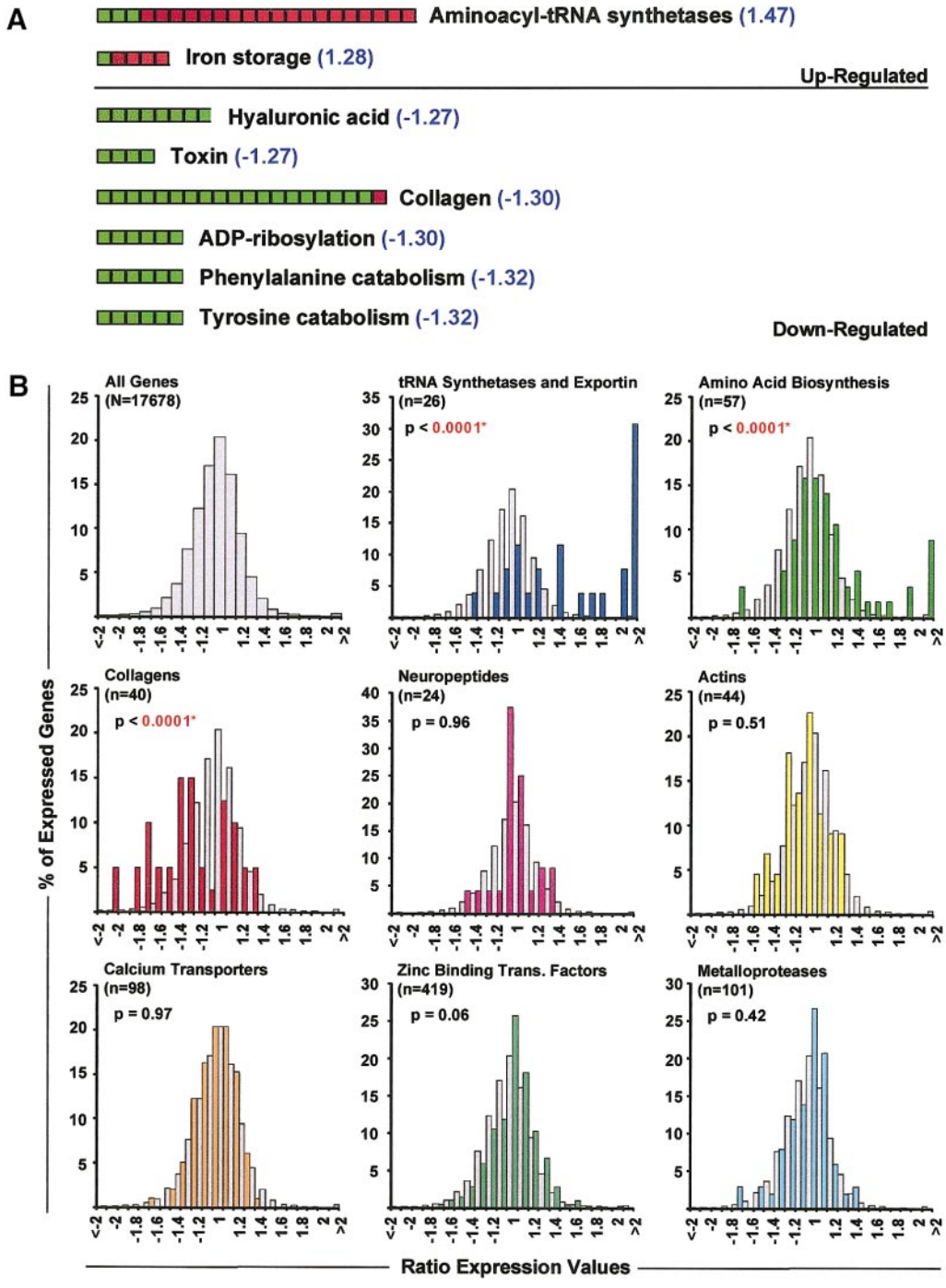

FIG. 5. (A) The DRAGON database was used to annotate all 17,678 genes analyzed on two Incyte microarrays with SWISS-PROT keyword information. The DRAGON Families information visualization tool was then used to visualize the ratio expression values of each keyword category across the entire data set. This analysis was used to identify groups of biologically related genes that are coordinately regulated. In the entire Incyte data set, one family (Aminoacyl-tRNA synthetase) was significantly, differentially up-regulated by lead treatment and one was found to be significantly down-regulated (Collagen) according to the criteria described under Results. Other families that were coordinately regulated but did not meet the criteria are also shown. The average expression value for each family is displayed in parentheses (blue text) to the right of each family. (B) The significance of the differential regulation of these two families was further investigated by comparing the distribution of all 17,678 gene expression values versus each gene family as defined by the "default hierarchy nodes" provided by GEMtools. Only three such families were found to have significantly altered distributions: tRNA synthetases and Exportin, Amino Acid Biosynthesis, and Collagens. The gray bars in each graph display the distribution of all gene expression values as shown in All Genes. The colored bars in each graph display the distribution of all of the genes in that family (e.g., Amino Acid Biosynthesis), the number in parentheses provides the number of genes in that family (e.g., $n = 57$), and the p values indicate the probability of a given distribution happening by chance as determined by χ^2 analysis. Significant p values ($p < 0.0001$) are displayed in red.

2000). We suggest that we have done so with lead in astrocyte cell cultures. Our ability to distinguish lead versus control and sodium samples purely through the clustering of microarray data is an example of the detection and use of a signature derived from gene expression data in order to identify toxicant- versus nontoxicant-treated cells. Results from our clustering analysis indicate that lead treatment of astrocyte cell cultures can induce a pattern of gene expression that is distinct from the normal profile of gene expression in that cell type. This pattern was consistent across four independent replicates of the lead-exposed cell cultures. However, we are not able to conclude whether the signature induced by lead is different from a signature that might be induced by other heavy metals (e.g., cadmium or mercury) or other nonmetal toxicants (e.g., pesticides). In order to conclude this, further microarray research comparing the pattern of gene expression induced by numerous toxicants is required. Furthermore, the signature we have identified in our studies is specific to astrocyte cell cultures and would presumably be partially or completely different in other cell cultures or tissue samples. Further studies are required to assess how similar the lead signature is across different species, tissues, developmental stages, lead concentrations, and time courses.

The distinct pattern of gene expression induced by lead and detected by our clustering methods is composed of the altered regulation of numerous specific genes. Many of these genes can be categorized into groups based upon shared properties.

Stress Response Genes

Of those genes found to be up-regulated by lead treatment on the Clontech microarrays, GFAP, microsomal glutathione *S*-transferase, mitochondrial 10-kDa heat shock protein, and HSP70 are all involved in general cellular responses to stress. In addition to VEGF (discussed below), a couple of these genes provide proof of principle for our microarray data. Specifically, both GFAP and HSP70 have both been previously reported to be differentially regulated by lead treatment. GFAP was found to be down-regulated in lead-treated astrocytes on both the Clontech and Incyte microarrays. On the Clontech Neuroarrays the lead versus control ratio was −1.8 with a *t* test *p* value of 0.00065 and the lead versus sodium ratio was −1.6 with a *t* test *p* value of 0.00032. On the Incyte microarray, while GFAP was found to be down-regulated, the degree of down-regulation was not as high. In the lead versus control samples, GFAP was down-regulated by a ratio of −1.3 and in the lead versus sodium samples it was down-regulated by a ratio of −1.1. Previous studies have reported the up-regulation (Stoltenburg *et al.,* 1996), down-regulation (Zawia and Harry, 1996), and altered regulation (Harry *et al.,* 1996) of GFAP following lead treatment in a range of tissues. HSP70 was differentially regulated on the Incyte arrays where it was represented by two different "spots" that were both among the top five most differentially regulated genes (HSP70 was not represented on

TABLE 3

Three Gene Families, tRNA Synthetases, Collagens, and Amino Acid Biosynthesis, Found To Be Significantly Coordinately Regulated on the Incyte Microarrays

PvC	PvN	Name	Genbank no.
		tRNA charging	
2.3	2.7	Methionine-tRNA synthetase	BE299937
2.2	2.9	Glutamyl-prolyl-tRNA synthetase	NM_004446
2.2	2.3	Tyrosyl-tRNA synthetase	U89436
2.1	1.7	Isoleucine-tRNA synthetase	U04953
2	2.2	Exportin, tRNA (nuclear exporter for tRNAs)	NM_007235
2	1.8	Threonyl-tRNA synthetase	M63180
1.4	1.6	Cysteinyl-tRNA synthetase	AA443954
1.2	1.4	Aspartyl-tRNA synthetase	NM_001349
1.2	1.4	Alanyl-tRNA synthetase	NM_001605
−1	1.1	Glutaminyl-tRNA synthetase	AA312973
−1	−1.1	Phenylalanine-tRNA synthetase-like	NM_004461
−1	−1.2	Arginyl-tRNA synthetase	S80343
−1.1	−1.4	Phenylalanine-tRNA synthetase-like	AW872787
		Collagens	
−2	−1.8	Collagen, type II, alpha 1	AW410427
−2	−1.6	Collagen, type XI, alpha 1	J04177
−1.8	−1.2	Collagen, type IV, alpha 1	M26576
−1.7	−1.7	Collagen, type V, alpha 2	Y14690
−1.7	−1.3	Collagen, type VIII, alpha 1	NM_001850
−1.7	−1.1	Collagen, type XIII, alpha 1	AW074709
−1.6	−1.4	Collagen, type IV, alpha 4	NM_000092
−1.5	−1.4	Collagen, type XV, alpha 1	L01697
−1.4	−1.5	Collagen, type XIX, alpha 1	AB004628
−1.4	−1.4	Collagen, type IX, alpha 3	L41162
−1.3	−1.4	Collagen, type I, alpha 1	AW577407
−1.3	−1.3	Collagen, type XVI, alpha 1	M92642
−1.3	−1.3	Collagen, type IX, alpha 1	AW022764
−1.2	−1	Adipose abundant gene transcript 1	D45371
−1	1.1	Collagen, type XVIII, alpha 1	AF018082
−1	1.1	Collagen, type IV, alpha 6	D21337
1.1	−1	Collagen, type VII, alpha 1	NM_000094
1.1	1.2	Adipose specific 2	AI093004
1.2	1.3	Collagen, type VI, alpha 1	X99135
1.3	−1	Collagen, type IV, alpha 3	M81379
		Amino acid biosynthesis	
2.7	3.1	Serine hydroxymethyltransferase 2	NM_005412
2.4	2.4	Methylene tetrahydrofolate dehydrogenase	NM_006636
2.2	1.9	Branched chain aminotransferase 1	AI970531
1.6	1.9	Argininosuccinate lyase	AA126106
1.3	1.4	Glutamic-oxaloacetic transaminase 2	NM_002080
−1.1	−1.2	Phosphoserine phosphatase-like	AL110317
−1.1	−1.2	Argininosuccinate synthetase	BE393272
−1.1	−1.1	Ornithine carbamoyltransferase	D00230
−1	−1	Tyrosine aminotransferase	NM_000353

Note. The regulation of each gene (name and Genbank no.) in a given family had similar expression levels on the lead versus control (PvC) and lead versus sodium (PvN) Incyte microarrays. All of the genes in the tRNA synthetases and Collagen families are shown. A subset of all genes in the Amino Acid Biosynthesis family is shown due to the size of the family. Genes that were down-regulated in lead-treated astrocytes are displayed with their ratio expression values with a grey background; genes that were up-regulated in lead-treated astrocytes have ratio expression values with a white background.

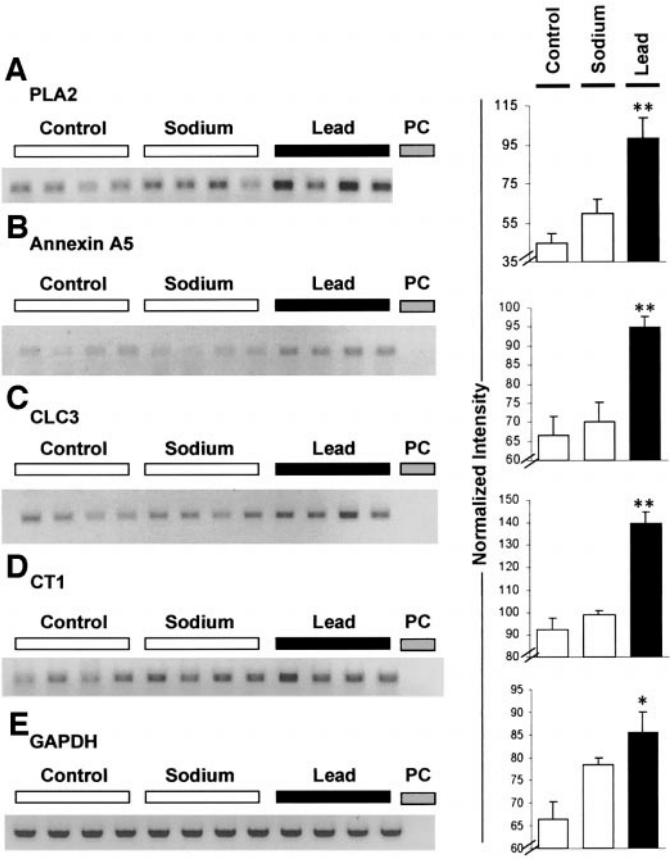

FIG. 6. Semiquantitative RT–PCR was used to confirm the differential regulation of four genes (phospholipase A2, PLA2; annexin A5; chloride channel 3, CLC3; and creatine transporter 1, CT1) compared to a nonregulated gene (glyceraldehyde-3-phosphate dehydrogenase, GAPDH) initially identified by Clontech and Incyte microarray analysis. Confirmations were performed in quadruplicate using cDNA samples from lead-, control-, and sodium-treated astrocytes. A primer control (PC) was run during each reaction in order to demonstrate specificity of the product. Band intensities were measured using Scion Image analysis software, normalized against corresponding GAPDH bands and averaged. Bar graphs to the right of each set of bands display average normalized values in addition to the standard deviation for each value. *Significant Student's *t* test value ($p < 0.05$) between lead and either control or sodium values. **Significant difference between lead and both of the other conditions. Results are typical of experiment performed three independent times, each time in quadruplicate.

the Clontech Neuroarrays). Altered levels of both HSP70 mRNA and protein have been detected in numerous previous studies (Selvin-Testa *et al.*, 1997; Witzmann *et al.*, 1999; Tully *et al.*, 2000). Another GST-related gene, Glutathione *S*-transferase like, was differentially regulated on the Incyte microarrays. All of these genes are found to be differentially regulated in response to a range of different cellular stressors, including UV irradiation, heat shock, other metal toxicants, and nonmetal toxicants. Therefore, the detection of the differential regulation of these genes on our microarrays suggests that the lead treatment we performed induces a general cellular stress response in astrocytes.

Genes Encoding Calcium Binding Proteins

Numerous genes encoding calcium binding proteins were differentially regulated by lead treatment including Ca^{2+}/calmodulin-activated adenlyl cyclase (Mons *et al.*, 1998), annexin A1, annexin A5, sorcin 22-kDa protein (Maki *et al.*, 1997; Brownawell and Creutz, 1997), calcineurin B subunit isoform 1, caldesmon 1, calmodulin-related protein NB-1, and two phospholipase A2 isoforms. Alteration of the transcriptional expression of genes that encode calcium binding proteins could be due to either indirect effects of lead on regulators of gene transcription (e.g., PKC or zinc-finger DNA binding proteins) or to the activation of regulatory feedback loops due to the direct binding of lead to calcium binding proteins. Our data do not allow us to distinguish between these two possible mechanisms.

Of the numerous differentially regulated genes known to encode calcium binding proteins, a few are particularly noteworthy. First, the phospholipase A2s are a family of C2-domain containing calcium-dependent phospholipid binding proteins. Lead has been previously shown to bind to the calcium binding C2 domain of synaptotagmin I (Bouton *et al.*, 2001). Therefore, it is possible that lead may also directly bind

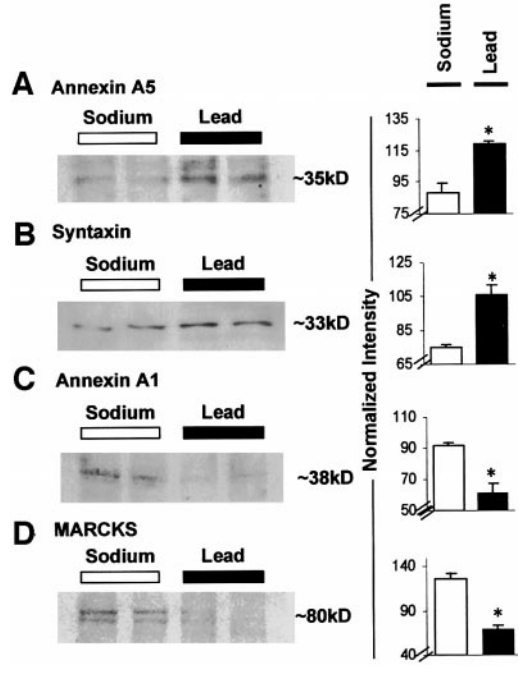

FIG. 7. Western blotting for four different proteins (annexin 1, annexin 5, syntaxin, and MARCKS) found to be differentially regulated at the RNA level by Clontech and Incyte microarray analysis. Western blots were conducted using detergent-solubilized, cytosolic cellular fractions of lead- versus sodium-treated astrocyte cell cultures. Samples were analyzed in duplicate. Band intensities were measured using Scion Image image analysis software, normalized to band intensities derived from Ponceau S staining (see Materials and Methods), averaged, and graphed to the right of each set of bands along with error bars representing standard deviation. Results are typical of an experiment performed three independent times, each time in duplicate.

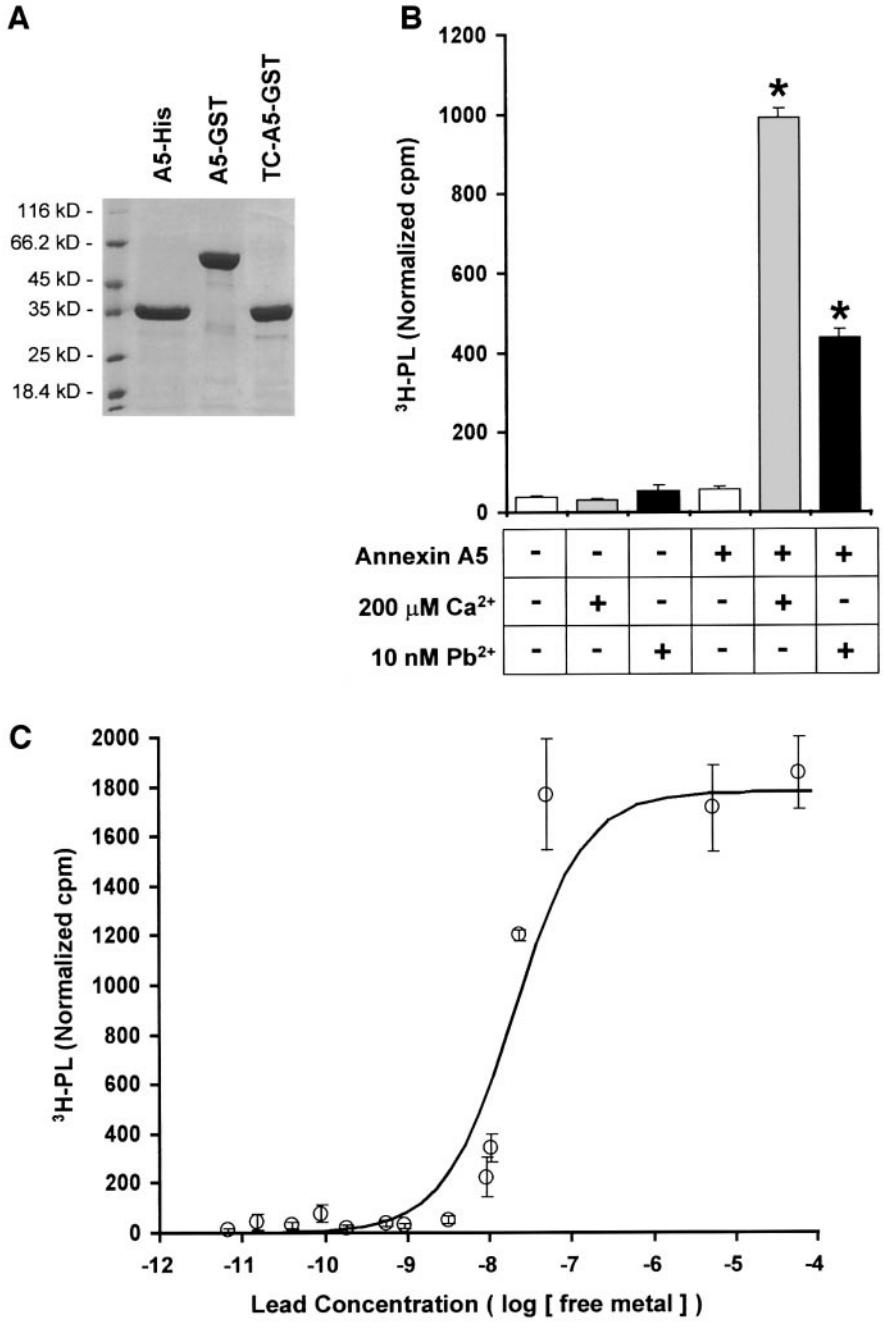

FIG. 8. (A) His-tagged annexin A5 (~35 kDa) was initially acquired from the laboratory of Dr. Mark Schlissel. This clone was used to produce a GST fusion of annexin A5 (~60 kDa) that was then thrombin-cleaved in order to obtain pure, unfused annexin A5 protein (~35 kDa). (B) Phospholipid binding reactions were carried out in the presence or absence of annexin A5 protein under three different cation conditions: no cation (1 mM NTA), calcium (200 μM Ca^{2+}), or lead (10 nM Pb^{2+}). Tritiated phospholipid scintillation counts were normalized as described under Materials and Methods. *Student's *t* test $p < 0.05$ for either calcium or lead condition versus no cation condition. Error bars indicate standard deviation. Results are typical of experiment performed three independent times, each time in triplicate. (C) Phospholipid binding reactions were carried out across a range of physiologically relevant free lead concentrations. The curve was fit to the data as described under Materials and Methods. An EC50 of ~30 nM was calculated for lead-dependent binding of annexin A5 to phospholipid liposomes. Error bars indicate standard deviation. Results are typical of experiment performed three independent times, each time in triplicate.

to PLA2 isoforms via their C2 domains. Previous studies have demonstrated either a direct activation of PLA2 by lead *in vitro* (Krug and Berndt, 1987; Krug *et al.*, 1994) or a ionophore-dependent activation of PLA2 by lead (Bressler *et al.*, 1994) as measured by increases in free arachidonic acid. Recently, Osterode and Ulberth (2000) demonstrated increased concentrations of arachidonic acid in the red blood cells (RBC) of 12 lead-exposed adult men compared to 12 healthy, unexposed,

age-matched adult men, suggesting that the effects of lead on PLA2 can also occur *in vivo* in lead-exposed humans. The increases in arachidonic acid in the RBCs of the lead-exposed men were directly correlated with the concentration of lead in the blood of each individual.

Second, the annexin A5 gene, which encodes a calcium-dependent phospholipid binding protein (Meers *et al.,* 1991; Kohler *et al.,* 1997), was differentially regulated by lead. We hypothesized that the annexin A5 protein might be a direct molecular target of lead based upon previous data showing that lead binds to other calcium-dependent phospholipid binding proteins such as PKC and synaptotagmin I. Most members of the annexin protein family contain four repeated domains that bind negatively charged phospholipids in a calcium-dependent manner. We used biochemical methods to demonstrate that nanomolar concentrations of lead can induce the phospholipid binding activity of annexin A5. These experiments suggest that lead does bind annexin A5 directly. Further studies are required in order to evaluate the role of the lead-induced phospholipid binding of annexin A5 within the context of the overall effects of lead in cellular systems.

Although the functions of the annexins have not been fully elucidated, it seems that many are involved in signal transduction cascades and neuronal activity regulation. Annexin A5 has been shown to be a potent inhibitor of PKC activity (Schlaepfer *et al.,* 1992; Shibata *et al.,* 1992; Dubois *et al.,* 1996). Some studies have reported that the inhibition of PKC by annexin A5 occurs through a direct interaction (Schlaepfer *et al.,* 1992). Other studies have reported that inhibition occurs primarily through the competition of annexin A5 and PKC for phospholipid binding during calcium-dependent activation (Dubois *et al.,* 1998). Our findings, when considered in the context of this previous literature, suggest that the lead-dependent activation of annexin A5 binding to phospholipid liposomes may resemble the cellular effects of lead-dependent PKC activation.

Finally, Markovac and Goldstein (1988) previously demonstrated the activation of the calcium-binding protein PKC by picomolar concentrations of lead via the PKC C2 domain. Numerous subsequent studies have confirmed the alteration of PKC-dependent cellular systems by lead treatment. Alteration of PKC activity by the direct binding of lead to PKC can cause the altered transcriptional regulation of various genes. This may also occur because PKC aberrantly phosphorylates the protein products of these genes, leading to the altered protein activity and subsequent feedback regulation of the protein's mRNA transcript. Our microarray results suggest that both types of PKC-dependent gene regulation may be occurring due to lead exposure. For example, numerous genes, the protein products of which are known to be phosphorylated by PKC, were found to be differentially regulated by lead in our microarray data. Examples include MARCKS (Albert *et al.,* 1986; Aderem, 1992), chloride channel 3 (CLC3; Duan *et al.,* 1999), histidine decarboxylase (Hocker *et al.,* 1996), and annexin A1. Alternatively, Hossain *et al.* (2000) reported the PKC-dependent regulation of the VEGF gene by lead treatment. They demonstrated that differential VEGF gene expression occurred due to the altered ability of PKC to transcriptionally regulate VEGF mRNA production.

Angiogenesis and Blood–Brain Barrier-Related Genes

Astrocytes participate in the formation of the blood–brain barrier. Lead can cause significant disruptions in blood–brain barrier formation, especially in young children. As previously discussed, due to the role of VEGF in angiogenesis and the maintenance of the blood–brain barrier, the differential regulation of VEGF by lead implicated VEGF in the microvasculopathy associated with lead encephalopathy. In the extended list of lead-altered genes identified in our study, three other differentially regulated genes were identified that might also be involved in the lead-induced disruption of the blood–brain barrier. First, the VEGF receptor Vascular endothelial growth factor receptor 3 precursor (Table 1) was found to be up-regulated on the Clontech microarrays. Second, thrombospondin 2, down-regulated on the Incyte microarrays (Table 2), is a potent inhibitor of angiogenesis that opposes the angiogenic activity of VEGF isoforms in skin and tumor vascularization (Tokunaga *et al.,* 1999; Kazuno *et al.,* 1999; Streit *et al.,* 1999; Detmar, 2000a,b). Finally, ephrin receptors were found to be differentially regulated by lead. Ephrin type-B receptor 3 precursor was down-regulated and ephrin type-A receptor 2 precursor was up-regulated on the Clontech microarrays (Table 1). The ephrin receptors have been previously shown to be involved in the adhesive response of endothelial cells and the remodeling of blood vessels (Wilkinson, 2000).

The extracellular matrix is critical to the integrity of the blood–brain barrier. We identified the lead-induced altered regulation of a large number of collagen genes in astrocytes within the context of the expression patterns of ~9000 other genes. The collagen genes were the only family of genes that were found to be coordinately down-regulated by lead and some of the collagen genes were among the most down-regulated genes identified (Table 3). These results indicate that acute low-level lead treatment has significant effects on the regulation of collagen genes as a group in astrocytes. Lead-induced alteration of collagen biosynthesis in astrocytes has potential implications for the effects of lead on the blood–brain barrier as suggested by previous studies (Rodolfo-Sioson and Ahrens, 1980). Effects of lead on collagen biosynthesis have also been studied in relation to rheumatoid arthritis (Goldberg *et al.,* 1983), skeletal abnormalities (Pounds *et al.,* 1991; Klein and Wiren, 1993; Hicks *et al.,* 1996), and lead-based skin ointments (Vandeputte *et al.,* 1990). One of the major sites of lead storage in the body is in bone. Lead is incorporated into bone during the calcification of cartilage (Hicks *et al.,* 1996) and can cause abberrant calcification of cartilaginous areas if injected subcutaneously (Ellender and Ham, 1987; Vandeputte *et al.,* 1990). Cartilage is made primarily of collagen. Lead also

binds to collagen (Miksik *et al.,* 1999). Previous studies have demonstrated lead-induced alterations in collagen biosynthesis at both the mRNA and protein level *in vitro* (Vistica *et al.,* 1977; Goldberg *et al.,* 1983; Long and Rosen, 1992; Klein and Wiren, 1993; Hicks *et al.,* 1996) and *in vivo* (Rodolfo-Sisoson and Ahrens, 1980; Rana and Prakash, 1986; Ahrens, 1993). The effects of lead on collagen biosynthesis have been linked to calcium-dependent signaling pathways that include PKC and EGF (Pounds *et al.,* 1991; Long and Rosen, 1992).

Amino Acid Biosynthesis and tRNA Synthetases

Studies five decades ago first reported the cleavage of ribonucleic acids by lead (Dimroth *et al.,* 1950; Farkas, 1968). Since then, lead has been routinely used as a tool for the study of the secondary structure of tRNA (Krebs *et al.,* 1972; Farkas *et al.,* 1972; Pan *et al.,* 1994; Otzen *et al.,* 1994; Ciesiolka *et al.,* 1998; Perreau *et al.,* 1999), mRNA (Farkas, 1975), and rRNA molecules (Winter *et al.,* 1997). Lead is capable of cleaving RNA at specific sites through a mechanism of nucleophilic attack (Brown *et al.,* 1983). Low micromolar concentrations of lead can cause RNA cleavage (Werner *et al.,* 1976). Lead-induced RNA cleavage can occur both *in vitro* and *in vivo* (Kennedy *et al.,* 1983). Under physiological conditions (pH 7.4 and 37°C) lead is 28 times more potent than the next most effective divalent cation, zinc, in cleaving RNA (Farkas, 1968; Otzen *et al.,* 1994). Kennedy *et al.* (1983) prepared postmitochondrial fractions from the brains of rat pups treated with 4% lead carbonate maternal milk for 2 days. Lead-exposed fractions displayed significantly lower amounts of protein synthesis activity than controls. A significant reduction in the level of tRNA synthetase activity accounted for most of the reduction in protein synthesis activity. Our microarray results, when analyzed in relation to previous findings, indicate that the protein synthesis machinery is a target of lead treatment. This is suggested by the coordinate differential regulation of the amino acid biosynthesis-related genes (Table 3). Furthermore, it seems that tRNA synthetase activity in particular is disrupted by lead and that this ability to cleave tRNA molecules may be the cause of these disruptions. A reduction in the amount of tRNA available for the tRNA synthetases would cause a reduction in the synthase activity and thus impair protein synthesis. Exportin-t is the major nuclear exporter of tRNA molecules (Arts *et al.,* 1998a,b; Kutay *et al.,* 1998; Lipowsky *et al.,* 1999; Grosshans *et al.,* 2000) and was also found to be significantly up-regulated in lead-treated astrocytes.

Conclusions

We have employed cDNA microarrays to simultaneously detect the expression levels of ~10,000 genes in lead-exposed astrocytes. The data generated from this analysis allowed for observations regarding the effects of lead on gene expression patterns and the identification of several novel *in vitro* molecular targets of lead. First, using established clustering methods, we have demonstrated the ability to differentiate between lead-exposed versus two types of control-treated cells solely on the basis of gene expression patterns. This indicates that lead can induce a distinct pattern of gene expression in astrocytes. Second, as proof of principle, we have identified genes previously shown to be differentially regulated by lead. Third, we have identified novel putative targets of lead and have discussed the implications of these findings in relation to previous literature concerning the cellular effects of lead. Finally, based upon our microarray data, we hypothesized that a specific gene product, annexin A5 protein, may be a direct molecular target of lead. Subsequent biochemical studies demonstrated that lead induces the phospholipid binding of annexin A5 at nanomolar concentrations. Annexin A5 phospholipid binding is normally induced by calcium at micromolar concentrations. Therefore, lead is capable of disrupting the normal phospholipid binding characteristics of annexin A5 in a manner similar to its effects on both PKC and synaptotagmin I.

We suggest that endogenous cation substitution is a central mechanism of lead toxicity. Alteration of the normal activity of both calcium and zinc binding proteins can cause a variety of molecular and cellular perturbations, including disruptions in normal gene expression patterns as we have reported herein. These lead-induced dysfunctions presumably manifest as clinical features upon sufficiently high levels of lead exposure. Future studies analyzing the gene expression profiles induced by lead versus other metal and nonmetal toxicants may allow for the further identification of similarities and differences caused by various toxicants.

ACKNOWLEDGMENTS

We thank Karim Hyder for his assistance with RNA preparation and Clontech Neuroarray hybridization, Adam Resnick for help with the Lightcycler, and Dr. Mark Schlissel for kindly supplying us with recombinant His-tagged annexin A5 protein. We thank N. Varg for helpful conversations. This study was supported by NIEHS Grant 5 PO1-ES08131 to J.P. and J.L.

REFERENCES

Aderem, A. (1992). The MARCKS brothers: A family of protein kinase C substrates. *Cell* **71,** 713–716.

Afshari, C. A., Nuwaysir, E. F., and Barrett, J. C. (1999). Application of complementary DNA microarray technology to carcinogen identification, toxicology, and drug safety evaluation. *Cancer Res.* **59,** 4759–4760.

Ahrens, F. A. (1993). Effects of lead on glucose metabolism, ion flux, and collagen synthesis in cerebral capillaries of calves. *Am. J. Vet. Res.* **54,** 808–812.

Albert, K. A., Walaas, S. I., Wang, J. K., and Greengard, P. (1986). Widespread occurrence of "87 kDa," a major specific substrate for protein kinase C. *Proc. Natl. Acad. Sci. USA* **83,** 2822–2826.

Alizadeh, A. A., Eisen, M. B., Davis, R. E., Ma, C., Lossos, I. S., Rosenwald, A., Boldrick, J. C., Sabet, H., Tran, T., Yu, X., Powell, J. I., Yang, L., Marti, G. E., Moore, T., Hudson, J., Jr., Lu, L., Lewis, D. B., Tibshirani, R., Sherlock, G., Chan, W. C., Greiner, T. C., Weisenburger, D. D., Armitage, J. O., Warnke, R., Levy, R., Wilson, W., Grever, M. R., Byrd, J. C.,

Botstein, D., Brown, P. O., and Staudt, L. M. (2000). Distinct types of diffuse large B-cell lymphoma identified by gene expression profiling. *Nature* **403,** 503–511.

Arts, G. J., Fornerod, M., and Mattaj, I. W. (1998a). Identification of a nuclear export receptor for tRNA. *Curr. Biol.* **8,** 305–314.

Arts, G. J., Kuersten, S., Romby, P., Ehresmann, B., and Mattaj, I. W. (1998b). The role of exportin-t in selective nuclear export of mature tRNAs. *EMBO J.* **17,** 7430–7441.

Bartholdi, D., Rubin, B. P., and Schwab, M. E. (1997). VEGF mRNA induction correlates with changes in the vascular architecture upon spinal cord damage in the rat. *Eur. J. Neurosci.* **9,** 2549–2560.

Berg, J. (1990). Zinc fingers and other metal-binding domains. *J. Biol. Chem.* **265,** 6513–6516.

Berg, J. M., and Godwin, H. A. (1997). Lessons from zinc-binding peptides. *Annu. Rev. Biophys. Biomol. Struct.* **26,** 357–371.

Bergdahl, I. A., Grubb, A., Schutz, A., Desnick, R. J., Wetmur, J. G., Sassa, S., and Skerfving, S. (1997). Lead binding to gamma-aminolevulinic acid dehydratase (ALAD) in human erythrocytes. *Pharmacol. Toxicol.* **81,** 153–158.

Bielarczyk, H., Tian, X., and Suszkiw, J. B. (1996). Cholinergic denervation-like changes in rat hippocampus following developmental lead exposure. *Brain Res.* **708,** 108–115.

Bielarczyk, H., Tomsig, J. L., and Suszkiw, J. B. (1994). Perinatal low-level lead exposure and the septo-hippocampal cholinergic system: Selective reduction of muscarinic receptors and cholineacetyltransferase in the rat septum. *Brain Res.* **643,** 211–217.

Bouton, C. M., Frelin, L. P., Forde, C. E., Godwin, H. A., and Pevsner, J. (2001). Synaptotagmin I is a molecular target for lead. *J. Neurochem.* **76,** 1724–1735.

Bouton, C. M., and Pevsner, J. (2000a). DRAGON: Database Referencing of Array Genes Online. *Bioinformatics* **16,** 1038–1039.

Bouton, C. M., and Pevsner, J. (2000b). Effects of lead on gene expression. *Neurotoxicology* **21,** 1045–1055.

Bressler, J., Forman, S., and Goldstein, G. W. (1994). Phospholipid metabolism in neural microvascular endothelial cells after exposure to lead *in vitro*. *Toxicol. Appl. Pharmacol.* **126,** 352–360.

Bressler, J. P., and Goldstein, G. W. (1991). Mechanisms of lead neurotoxicity. *Biochem. Pharmacol.* **41,** 479–484.

Bressler, J., Kim, K., Chakraborti, T., and Goldstein, G. (1999). Molecular mechanisms of lead neurotoxicity. *Neurochem. Res.* **24,** 595–600.

Brown, R. S., Hingerty, B. E., Dewan, J. C., and Klug, A. (1983). Pb(II)-catalysed cleavage of the sugar-phosphate backbone of yeast $tRNA^{Phe}$—Implications for lead toxicity and self-splicing RNA. *Nature* **303,** 543–546.

Brownawell, A. M., and Creutz, C. E. (1997). Calcium-dependent binding of sorcin to the N-terminal domain of synexin (annexin VII). *J. Biol. Chem.* **272,** 22182–22190.

Burczynski, M. E., McMillian, M., Ciervo, J., Li, L., Parker, J. B., Dunn, R. T., Hicken, S., Farr, S., and Johnson, M. D. (2000). Toxicogenomics-based discrimination of toxic mechanism in HepG2 human hepatoma cells. *Toxicol. Sci.* **58,** 399–415.

Centers for Disease Control (1991). *Preventing Lead Poisoning in Young Children.* Centers for Disease Control, Atlanta.

Chakraborti, T., Kim, K. A., Goldstein, G. G., and Bressler, J. P. (1999). Increased AP-1 DNA binding activity in PC12 cells treated with lead. *J. Neurochem.* **73,** 187–194.

Chapman, E. R., and Jahn, R. (1994). Calcium-dependent interaction of the cytoplasmic region of synaptotagmin with membranes: Autonomous function of a single C2-homologous domain. *J. Biol. Chem.* **269,** 5735–5741.

Cheng, S. Y., Nagane, M., Huang, H. S., and Cavenee, W. K. (1997). Intracerebral tumor-associated hemorrhage caused by overexpression of the vascular endothelial growth factor isoforms VEGF121 and VEGF165 but not VEGF189. *Proc. Natl. Acad. Sci. USA* **94,** 12081–12087.

Choi, D. W., and Koh, J. Y. (1998). Zinc and brain injury. *Annu. Rev. Neurosci.* **21,** 347–375.

Chow, T. J., Patterson, C. C., and Settle, D. (1974). Occurrence of lead in tuna. *Nature* **251,** 159–161.

Chu, S., DeRisi, J., Eisen, M., Mulholland, J., Botstein, D., Brown, P. O., and Herskowitz, I. (1998). The transcriptional program of sporulation in budding yeast. *Science* **282,** 699–705.

Ciesiolka, J., Michalowski, D., Wrzesinski, J., Krajewski, J., and Krzyzosiak, W. J. (1998). Patterns of cleavages induced by lead ions in defined RNA secondary structure motifs. *J. Mol. Biol.* **275,** 211–220.

Clasen, R. A., Hartmann, J. F., Starr, A. J., Coogan, P. S., Pandolfi, S., Laing, I., Becker, R., and Hass, G. M. (1973). Electron microscopic and chemical studies of the vascular changes and edema of lead encephalopathy. A comparative study of the human and experimental disease. *Am. J. Pathol.* **74,** 215–240.

Davey, F. D., and Breen, K. C. (1998). Stimulation of sialytransferase by subchronic low-level lead exposure in the developing nervous system. *Toxicol. Appl. Pharmacol.* **151,** 16–21.

Davletov, B. A., and Sudhof, T. C. (1993). A single C2 domain from synaptotagmin I is sufficient for high affinity Ca2+/phospholipid binding. *J. Biol. Chem.* **268,** 26386–26390.

Detmar, M. (2000a). The role of VEGF and thrombospondins in skin angiogenesis. *J. Dermatol. Sci.* **24**(Suppl. 1), S78–S84.

Detmar, M. (2000b). Tumor angiogenesis. *J. Invest. Dermatol. Symp. Proc.* **5,** 20–23.

Dimroth, K., Jaenicke, L., and Heinzel, D. (1950). Die spaltung der pentosenucleinsaure der hefe mit bleihydroxyd. *Liebigs Ann. Chem.* **566,** 206–210.

Duan, D., Cowley, S., Horowitz, B., and Hume, J. R. (1999). A serine residue in CLC3 links phosphorylation-dephosphorylation to chloride channel regulation by cell volume. *J. Gen. Physiol.* **113,** 57–70.

Dubois, T., Mira, J. P., Feliers, D., Solito, E., Russo-Marie, F., and Oudinet, J. P. (1998). Annexin V inhibits protein kinase C activity via a mechanism of phospholipid sequestration. *Biochem. J.* **330,** 1277–1282.

Dubois, T., Oudinet, J. P., Mira, J. P., and Russo-Marie, F. (1996). Annexins and protein kinases C. *Biochim. Biophys. Acta* **1313,** 290–294.

Eisen, M. B., Spellman, P. T., Brown, P. O., and Botstein, D. (1998). Cluster analysis and display of genome-wide expression patterns. *Proc. Natl. Acad. Sci. USA* **95,** 14863–14868.

Ellender, G., and Ham, K. N. (1987). Connective tissue responses to some heavy metals. II. Lead: Histology and ultrastructure. *Br. J. Exp. Pathol.* **68,** 291–307.

Farkas, W. R. (1968). Depolymerization of ribonucleic acid by plumbous ion. *Biochim. Biophys. Acta* **26,** 401–409.

Farkas, W. R. (1975). Effect of plumbous ion on messenger RNA. *Chem.–Biol. Interact.* **11,** 253–263.

Farkas, W. R., Hewins, S., and Welch, J. W. (1972). Effects of plumbous ions on some functions of transfer RNA. *Chem.–Biol. Interact.* **5,** 191–200.

Ferrara, N., and Henzel, W. J. (1989). Vascular endothelial growth factor and the regulation of angiogenesis. *Biochem. Biophys. Res. Commun.* **161,** 851–858.

Finkelstein, Y., Markowitz, M. E., and Rosen, J. F. (1998). Low-level lead-induced neurotoxicology in children: An update on central nervous system effects. *Brain Res. Rev.* **27,** 168–176.

Foletta, V. C. (1996). Transcription factor AP-1, and the role of Fra-2. *Immunol. Cell. Biol.* **74,** 121–133.

Fullmer, C. S., Edelstein, S., and Wasserman, R. H. (1985). Lead-binding proteins of intestinal calcium-binding proteins. *J. Biol. Chem.* **260,** 6816–6819.

Gasch, A. P., Spellman, P. T., Kao, C. M., Carmel-Harel, O., Eisen, M. B., Storz, G., Botstein, D., and Brown, P. O. (2000). Genomic expression programs in the response of yeast cells to environmental changes. *Mol. Biol. Cell* **11,** 4241–4257.

Gnanadesikan, R. (Ed.) (1977). *Methods for Statistical Data Analysis of Multivariate Observations.* Wiley, New York.

Goering, P. L. (1993). Lead–protein interactions as a basis for lead toxicity. *Neurotoxicology* **14,** 45–60.

Goldberg, R. L., Kaplan, S. R., and Fuller, G. C. (1983). Effect of heavy metals on human rheumatoid synovial cell proliferation and collagen synthesis. *Biochem. Pharmacol.* **32,** 2763–2766.

Goldstein, G. W. (1992). Neurologic concepts of lead poisoning in children. *Pediatr. Ann.* **21,** 384–388.

Goldstein, G. W. (1993). Evidence that lead acts as a calcium substitute in second messenger metabolism. *Neurotoxicology* **14,** 97–101.

Goldstein, G. W., and Ar, D. (1983). Lead activates calicium sensitive processes. *Life Sci.* **33,** 1001–1006.

Goldstein, G. W., Asbury, A. K., and Diamond, I. (1974). Pathogenesis of lead encephalopathy. Uptake of lead and reaction of brain capillaries. *Arch. Neurol.* **31,** 382–389.

Goyer, R. A. (1996). Results of lead research: Prenatal exposure and neurological consequences. *Environ. Health Perspect.* **104,** 1050–1054.

Grosshans, H., Hurt, E., and Simos, G. (2000). An aminoacylation-dependent nuclear tRNA export pathway in yeast. *Genes Dev.* **14,** 830–840.

Guilarte, T. R. (1997). Glutamatergic system and developmental lead neurotoxicity. *Neurotoxicology* **18,** 665–672.

Haar, G. T. (1975). Lead in the environment—Origins, pathways and sinks. *Environ. Qual. Saf. Suppl.* **2,** 76–94.

Habermann, E., Crowell, K., and Janicki, P. (1983). Lead and other metals can substitute for Ca^{2+} in calmodulin. *Arch. Toxicol.* **54,** 61–70.

Hanas, J. S., Rodgers, J. S., Bantle, J. A., and Cheng, Y. G. (1999). Lead inhibition of DNA-binding mechanism of Cys(2)His(2) zinc finger proteins. *Mol. Pharmacol.* **56,** 982–988.

Harry, G. J., Schmitt, T. J., Gong, Z., Brown, H., Zawia, N. H., and Evans, H. L. (1996). Lead-induced alterations of glial fibrillary acidic protein (GFAP) in the developing rat brain. *Toxicol. Appl. Pharmacol.* **139,** 84–93.

Heyer, L. J., Kruglyak, S., and Yooseph, S. (1999). Exploring expression data: Identification and analysis of coexpressed genes. *Genome Res.* **9,** 1106–1115.

Hicks, D. G., O'Keefe, R. J., Reynolds, K. J., Cory-Slechta, D. A., Puzas, J. E., Judkins, A., and Rosier, R. N. (1996). Effects of lead on growth plate chondrocyte phenotype. *Toxicol. Appl. Pharmacol.* **140,** 164–172.

Hocker, M., Zhang, Z., Fenstermacher, D. A., Tagerud, S., Chulak, M., Joseph D., and Wang, T. C. (1996). Rat histidine decarboxylase promoter is regulated by gastrin through a protein kinase C pathway. *Am. J. Physiol.* **270,** G619–G633.

Hossain, M. A., Bouton, C. M., Pevsner, J., and Laterra, J. (2000). Induction of vascular endothelial growth factor in human astrocytes by lead. *J. Biol. Chem.* **275,** 27874–27882.

Janknecht, R., Cahill, M. A., and Nordheim, A. (1995). Signal integration at the c-*fos* promoter. *Carcinogenesis* **16,** 443–450.

Johnson, F. M. (1998). The genetic effects of environmental lead. *Mutat. Res.* **410,** 123–140.

Kazuno, M., Tokunaga, T., Oshika, Y., Tanaka, Y., Tsugane, R., Kijima, H., Yamazaki, H., Ueyama, Y., and Nakamura, M. (1999). Thrombospondin-2 (TSP2) expression is inversely correlated with vascularity in glioma. *Eur. J. Cancer* **35,** 502–506.

Kennedy, J. L., Girgis, G. R., Rakhra, G. S., and Nicholls, D. M. (1983). Protein synthesis in rat brain following neonatal exposure to lead. *J. Neurol. Sci.* **59,** 57–68.

Kim, K., Annadata, M., Goldstein, G. W., and Bressler, J. P. (1997). Induction of c-fos mRNA by lead in PC12 cells. *Int. J. Dev. Neurosci.* **15,** 175–182.

Kim, K., Chakraborti, T., Goldstein, G. W., and Bressler, J. P. (2000). Immediate early gene expression in PC12 cells exposed to lead: Requirement for protein kinase C. *J. Neurochem.* **74,** 1140–1146.

Klein, R. F., and Wiren, K. M. (1993). Regulation of osteoblastic gene expression by lead. *Endocrinology* **132,** 2531–2537.

Kohler, G., Hering, U., Zschornig, O., and Arnold, K. (1997). Annexin V interaction with phosphatidylserine-containing vesicles at low and neutral pH. *Biochemistry* **36,** 8189–8194.

Krebs, B., Werner, C., and Dirheimer, G. (1972). Action of divalent lead on phenylalanine tRNA of brewer's yeast. *Eur. J. Toxicol. Hyg. Environ.* **5,** 337–342.

Krug, H., and Berndt, J. (1987). Stimulation of arachidonic acid metabolism via phospholipase A2 by triethyl lead. *Eur. J. Biochem.* **162,** 293–298.

Krug, H. F., Mattern, D., Bidault, J., and Ninio, E. (1994). Effects of organometals on cellular signaling. II. Inhibition of reincorporation of free arachidonic acid and influence on paf-acether synthesis by triethylead. *Environ. Health Perspect.* **102**(Suppl. 3), 331–334.

Kutay, U., Lipowsky, G., Izaurralde, E., Bischoff, F. R., Schwarzmaier, P., Hartmann, E., and Gorlich, D. (1998). Identification of a tRNA-specific nuclear export receptor. *Mol. Cell* **1,** 359–369.

Landrigan, P. J., and Todd, A. C. (1994). Lead poisoning. *West. J. Med.* **161,** 153–159.

Laterra, J., Bressler, J. P., Indurti, R. R., Belloni-Olivi, L., and Goldstein, G. W. (1992). Inhibition of astroglia-induced endothelial differentiation by inorganic lead: A role for protein kinase C. *Proc. Natl. Acad. Sci. USA* **89,** 10748–10752.

Leung, D. W., Cachianes, G., Kuang, W. J., Goeddel, D. V., and Ferrara, N. (1989). Vascular endothelial growth factor is a secreted angiogenic mitogen. *Science* **246,** 1306–1309.

Lipowsky, G., Bischoff, F. R., Izaurralde, E., Kutay, U., Schafer, S., Gross, H. J., Beier, H., and Gorlich, D. (1999). Coordination of tRNA nuclear export with processing of tRNA. *RNA* **5,** 539–549.

Long, G. J., and Rosen, J. F. (1992). Lead perturbs epidermal growth factor (EGF) modulation of intracellular calcium metabolism and collagen synthesis in clonal rat osteoblastic (ROS 17/2.8) cells. *Toxicol. Appl. Pharmacol.* **114,** 63–70.

Maki, M., Narayana, S. V., and Hitomi, K. (1997). A growing family of the Ca^{2+}-binding proteins with five EF-hand motifs. *Biochem. J.* **328,** 718–720.

Manalis, R. S., Cooper, G. P., and Pomeroy, S. L. (1984). Effects of lead on neuromuscular transmission in the frog. *Brain Res.* **294,** 95–109.

Manea-Krichten, M., Patterson, C., Miller, G., Settle, D., and Erel, Y. (1991). Comparative increases of lead and barium with age in human tooth enamel, rib and ulna. *Sci. Total Environ.* **107,** 179–203.

Markovac, J., and Goldstein, G. (1988). Picomolar concentrations of lead stimulate brain protein kinase C. *Nature* **334,** 71–73.

Martell, A. E., and Smith, R. M. (1989). Critical Stability Constants. Vol. 1. Plenum Press, New York, NY.

Marton, M. J., DeRisi, J. L., Bennett, H. A., Iyer, V. R., Meyer, M. R., Roberts, C. J., Stoughton, R., Burchard, J., Slade, D., Dai, H., Bassett, D. E., Hartwell, L. H., Brown, P. O., and Friend, S. H. (1998). Drug target validation and identification of secondary drug target effects using DNA microarrays. *Nat. Med.* **4,** 1293–1301.

Meers, P., Daleke, D., Hong, K., and Papahadjopoulos, D. (1991). Interactions of annexins with membrane phospholipids. *Biochemistry* **30,** 2903–2908.

Mielke, H. W., and Reagan, P. L. (1998). Soil is an important pathway of human lead exposure. *Environ. Health Perspect.* **1,** 217–229.

Miksik, I., Deyl, Z., Herget, J., Novotna, J., and Mestek, O. (1999). Binding of

lead to collagen type I and V and alpha2(I) CNBr(3,5) fragment by a modified Hummel-Dreyer method. *J. Chromatogr. A* **852,** 245–253.

Mira, J. P., Dubois, T., Oudinett, J. P., Lukowski, S., Russo-Marie, F., and Geny, B. (1997). Inhibition of cytosolic phospholipase A2 by annexin V in differentiated permeabilized HL-60 cells. *J. Biol. Chem.* **272,** 10474–10482.

Mirnics, K., Middleton, F. A., Marquez, A., Lewis, D. A., and Levitt, P. (2000). Molecular characterization of schizophrenia viewed by microarray analysis of gene expression in prefrontal cortex. *Neuron* **28,** 53–67.

Mons, N., Decorte, L., Jaffard, R., and Cooper, D. M. F. (1998). Ca^{2+}-sensitive adenlyl cyclases, key integrators of cellular signalling. *Life Sci.* **62,** 1647–1652.

Mushak, P., and Crocetti, A. F. (1989). Determination of numbers of lead-exposed American children as a function of lead source: Integrated summary of a report to the U.S. Congress on childhood lead poisoning. *Environ. Res.* **50,** 210–229.

Needleman, H. L. (1994). Childhood lead poisoning. *Curr. Opin. Neurol.* **7,** 187–190.

Needleman, H. L. (1998). Childhood lead poisoning: The promise and abandonment of primary prevention. *Am. J. Public Health* **88,** 1871–1877.

Needleman, H. L., Schell, A., Bellinger, D., Leviton, A., and Allred, E. N. (1990). The long-term effects of exposure to low doses of lead in childhood. *N. Engl. J. Med.* **322,** 83–88.

Nuwaysir, E. F., Bittner, M., Trent, J., Barrett, J. C., and Afshari, C. A. (1999). Microarrays and toxicology: The advent of toxicogenomics. *Mol. Carcinogen.* **24,** 153–159.

Osterode, W., and Ulberth, F. (2000). Increased concentration of arachidonic acid in erythrocyte membranes in chronically lead-exposed men. *J. Toxicol. Environ. Health* **59,** 87–95.

Otzen, D. E., Barciszewski, J., and Clark, B. F. C. (1994). Dual hydrolytic role for Pb(II) ions. *Biochimie* **76,** 15–21.

Ouyang, H., and Vogel, H. J. (1998). Metal ion binding to calmodulin: NMR and fluorescence studies. *Biometals* **11,** 213–222.

Pan, T., Dichtl, B., and Uhlenbeck, O. C. (1994). Properties of an in vitro selected Pb^{2+} cleavage motif. *Biochemistry* **33,** 9561–9565.

Patterson, C., and Settle, D. (1993). New mechanisms in lead biodynamics at ultra-low levels. *Neurotoxicology* **14,** 291–299.

Payne, J. C., Horst, M. A., and Godwin, H. A. (1999). Lead fingers: Pb^{2+} binding to structural zinc-binding domains determined directly by monitoring lead-thiolate charge-transfer bands. *J. Am. Chem. Soc.* **121,** 6850–6855.

Pennypacker, K. R., Xiao, Y., Xu, R. H., and Harry, G. J. (1997). Lead-induced developmental changes in AP-1 DNA binding in rat brain. *Int. J. Dev. Neurosci.* **15,** 321–328.

Perreau, V. M., Keith, G., Holmes, W. M., Przykorska, A., Santos, M. A. S., and Tuite, M. F. (1999). The *Candida albicans* CUG-decoding ser-tRNA has an atypical anticodon stem–loop structure. *J. Mol. Biol.* **293,** 1039–1053.

Pounds, J. G., Long, G. J., and Rosen, J. F. (1991). Cellular and molecular toxicity of lead in bone. *Environ. Health Perspect.* **91,** 17–32.

Press, M. F. (1977). Lead encephalopathy in neonatal Long-Evans rats: Morphologic studies. *J. Neuropathol. Exp. Neurol.* **36,** 169–193.

Rana, S. V., and Prakash, R. (1986). Collagen in the liver of metal fed rats. *Exp. Pathol.* **29,** 193–195.

Rocha, J. B. T., Pereira, M. E., Emanuelli, T., Christofari, R. S., and Souza, D. O. (1995). Effect of treatment with mercury chloride and lead acetate during the second stage of rapid postnatal brain growth on gamma-aminolevulinic acid dehydratase (ALAD) activity in brain, liver, kidney and blood of suckling rats. *Toxicology* **100,** 27–37.

Rockett, J. C., and Dix, D. J. (1999). Application of DNA array to toxicology. *Environ. Health Perspect.* **107,** 681–685.

Rodolfo-Sisoson, S. A., and Ahrens, F. A. (1980). The effects of lead on collagen biosynthesis in neonatal rats. *Res. Commun. Chem. Pathol. Pharmacol.* **29,** 317–328.

Romieu, I., Lacasana, M., and McConnell, R. (1997). Lead exposure in Latin America and the Caribbean. Lead Research Group of the Pan-American Health Organization. *Environ. Health Perspect.* **105,** 398–405.

Russo-Marie, F. (1999). Annexin V and phospholipid metabolism. *Clin. Chem. Lab. Med.* **37,** 287–291.

Sandhir, R., and Gill, K. (1994a). Calmodulin and cAMP dependent synaptic vesicle protein phosphorylation in rat cortex following lead exposure. *Int. J. Biochem.* **26,** 1383–1389.

Sandhir, R., and Gill, K. D. (1994b). Effect of lead on the biological activity of calmodulin in rat brain. *Exp. Mol. Pathol.* **61,** 69–75.

Sandhir, R., and Gill, K. D. (1994c). Lead perturbs calmodulin dependent cyclic AMP metabolism in rat central nervous system. *Biochem. Mol. Biol. Int.* **33,** 729–742.

Schlaepfer, D. D., Jones, J., and Haigler, H. T. (1992). Inhibition of protein kinase C by annexin V. *Biochemistry* **31,** 1886–1891.

Schmitt, T. J., Zawia, N., and Harry, G. J. (1996). GAP-43 mRNA expression in the developing rat brain: Alterations following lead-acetate exposure. *Neurotoxicology* **17,** 407–414.

Schoenmakers, T. J., Visser, G. J., Flik, G., and Theuvenet, A. P. (1992). CHELATOR: An improved method for computing metal ion concentrations in physiological solutions. *Biotechniques* **12,** 874.

Selvin-Testa, A., Capani, F., Loidl, C. F., Lopez, E. M., and Pecci-Saavedra, J. (1997). Prenatal and postnatal lead exposure induces 70 kDa heat shock protein in young rat brain prior to changes in astrocyte cytoskeleton. *Neurotoxicology* **18,** 805–817.

Settle, M., and Patterson, C. C. (1980). Lead in albacore: Guide to lead pollution in Americans. *Science* **207,** 1167–1176.

Shibata, S., Sato, H., and Maki, M. (1992). Calphobindin I (annexin V) inhibits protein kinase C. *Tohoku J. Exp. Med.* **166,** 479–481.

Simons, T. J. B. (1993). Lead-calcium interactions in cellular lead toxicity. *Neurotoxicology* **14,** 77–86.

Spellman, P. T., Sherlock, G., Zhang, M. Q., Iyer, V. R., Anders, K., Eisen, M. B., Brown, P. O., Botstein, D., and Futcher, B. (1998). Comprehensive identification of cell cycle-regulated genes of the yeast *Saccharomyces cerevisiae* by microarray hybridization. *Mol. Biol. Cell* **9,** 3273–3297.

Stoltenburg, G., Punder, I., Peters, B., Marcinkowski, M., Herbst, H., Winneke, G., and Wiegand, H. (1996). Glial fibrillary acidic protein and RNA expression in adult rat hippocampus following low-level lead exposure during development. *Histochem. Cell. Biol.* **105,** 431–442.

Streit, M., Riccardi, L., Velasco, P., Brown, L. F., Hawighorst, T., Bornstein, P., and Detmar, M. (1999). Thrombospondin 2: A potent endogenous inhibitor of tumor growth and angiogenesis. *Proc. Natl. Acad. Sci. USA* **96,** 14888–14893.

Suzuki, T., Morimura, S., Diccianni, M. B., Yamada, R., Hochi, S. I., Hirabayashi, M., Yuki, A., Nomura, K., Kitagawa, T., Imagawa, M., and Muramatsu, M. (1996). Activation of glutathione transferase P gene by lead requires glutathione transferase P enhancer I. *J. Biol. Chem.* **271,** 1626–1632.

Tian, X., Sun, X., and Suszkiw, J. B. (1996). Developmental age-dependent upregulation of choline acetyltransferase and vesicular acetylcholine transporter mRNA expression in neonatal rat septum by nerve growth factor. *Neurosci. Lett.* **209,** 134–136.

Tian, X., Sun, X., and Suszkiw, J. B. (2000). Upregulation of tyrosine hydroxylase and downregulation of choline acetyltransferase in lead-exposed PC12 cells: The role of PKC activation. *Toxicol. Appl. Pharmacol.* **167,** 246–252.

Tiffany-Castiglioni, E. (1993). Cell culture models for lead toxicity in neuronal and glial cells. *Neurotoxicology* **14,** 513–536.

Tokunaga, T., Nakamura, M., Oshika, Y., Abe, Y., Ozeki, Y., Fukushima, Y.,

Hatanaka, H., Sadahiro, S., Kijima, H., Tsuchida, T., Yamazaki, H., Tamaoki, N., and Ueyama, Y. (1999). Thrombospondin 2 expression is correlated with inhibition of angiogenesis and metastasis of colon cancer. *Br. J. Cancer* **79,** 354–359.

Tomsig, J. L., and Suszkiw, J. B. (1990). Pb^{2+}-induced secretion from bovine chromaffin cells: Fura-2 as a probe for Pb^{2+}. *Am. J. Physiol.* **259,** C762–C768.

Tomsig, J. L., and Suszkiw, J. B. (1993). Intracellular mechanism of $Pb^{(2+)}$-induced norepinephrine release from bovine chromaffin cells. *Am. J. Physiol.* **265,** C1630–C1636.

Tomsig, J. L., and Suszkiw, J. B. (1995). Multisite interactions between Pb^{2+} and protein kinase C and its role in norepinephrine release from bovine adrenal chromaffin cells. *J. Neurochem.* **64,** 2667–2673.

Tully, D. B., Collins, B. J., Overstreet, J. D., Smith, C. S., Dinse, G. E., Mumtaz, M. M., and Chapin, R. E. (2000). Effects of arsenic, cadmium, chromium, and lead on gene expression regulated by a battery of 13 different promoters in recombinant HepG2 cells. *Toxicol. Appl. Pharmacol.* **168,** 79–90.

Vandeputte, D. F., Jacob, W. A., and Van Grieken, R. E. (1990). Phosphorous, calcium and distribution in collagen in lead induced soft tissue calcification. An ultrastructural and X-ray microanalytical study. *Matrix* **10,** 33–37.

Vistica, D. T., Ahrens, F. A., and Ellison, W. R. (1977). The effects of lead upon collagen synthesis and proline hydroxylation in the Swiss mouse 3T6 fibroblast. *Arch. Biochem. Biophys.* **179,** 15–23.

Warren, M. J., Cooper, J. B., Wood, S. P., and Shoolingin-Jordan, P. M. (1998). Lead poisoning, haem synthesis and 5-aminolaevulinic acid dehydratase. *TIBS* **23,** 217–221.

Wen, X., Fuhrman, S., Michaels, G. S., Carr, D. B., Smith, S., Barker, J. L., and Somogyi, R. (1998). Large-scale temporal gene expression mapping of central nervous system development. *Proc. Natl. Acad. Sci. USA* **95,** 334–339.

Werner, C., Krebs, B., Keith, G., and Dirheimer, G. (1976). Specific cleavages of pure tRNAs by plumbous ions. *Biochim. Biophys. Acta* **432,** 161–175.

Wilkinson, D. G. (2000). Eph receptors and ephrins: Regulators of guidance and assembly. *Int. Rev. Cytol.* **196,** 177–244.

Wilson, M., DeRisi, J., Kristensen, H. H., Imboden, P., Rane, S., Brown, P. O., and Schoolnik, G. K. (1999). Exploring drug-induced alterations in gene expression in *Mycobacterium tuberculosis* by microarray hybridization. *Proc. Natl. Acad. Sci. USA* **96,** 12833–12838.

Winter, D., Polacek, N., Halama, I., Streicher, B., and Barta, A. (1997). Lead-catalyzed specific cleavage of ribosomal RNAs. *Nucleic Acid Res.* **25,** 1817–1824.

Witzmann, F. A., Fultz, C. D., Grant, R. A., Wright, L. S., Kornguth, S. E., and Siegel, F. L. (1999). Regional protein alterations in rat kidneys induced by lead exposure. *Electrophoresis* **20,** 943–951.

Zawia, N. H., and Harry, G. J. (1996). Developmental exposure to lead interferes with glial and neuronal differential gene expression in the rat cerebellum. *Toxicol. Appl. Pharmacol.* **138,** 43–47.

Zawia, N. H., Sharan, R., Brydie, M., Oyama, T., and Crumpton, T. (1998). Sp1 as a target site for metal-induced perturbations of transcriptional regulation of developmental brain gene expression. *Dev. Brain Res.* **107,** 291–298.

Zhu, Z., and Thiele, D. J. (1996). Toxic metal-responsive gene transcription. *EXS* **77,** 307–320.